NATIONAL ADVISORY COMMITTEE FOR AERONAUTICS

TECHNICAL NOTE 4036

CREEP OF ALUMINUM-COPPER ALLOYS DURING AGE HARDENING

By E. E. Underwood, L. L. Marsh, and G. K. Manning

Battelle Memorial Institute

Washington

February 1958

NATIONAL ADVISORY COMMITTEE FOR AERONAUTICS

TECHNICAL NOTE 4036

CREEP OF ALUMINUM-COPPER ALLOYS DURING AGE HARDENING

By E. E. Underwood, L. L. Marsh, and G. K. Manning

SUMMARY

The interrelation of aging during creep and of creep during aging has been studied in polycrystalline aluminum alloys containing 1 to 4 percent copper. Experimental procedures included interrupted creep tests, tensile tests of crept specimens, quantitative metallographic determination of the percent precipitation during creep, hardness measurements on unstressed and stressed aged alloys, X-ray studies of deformation in the crystalline lattice, and microscopic examination of the surface-deformation markings.

Aging of 2-percent-copper alloys under stress resulted in two to three times more precipitation than there was in unstressed samples. The maximum measured amount of precipitation was about 10 times greater than that indicated by the phase diagram - assuming the equilibrium precipitate. A review of the pertinent literature suggested that the solute concentration of the "initial" precipitate could be less than that generally assumed, and a calculation based on dilatometric measurements gave a figure that agreed closely with the measured maximum amount of precipitation.

Hardness measurements on unstressed aged alloys yielded curves of constant time to maximum hardness and curves of constant maximum hardness over a range of temperatures and compositions. When these curves are superimposed on the phase diagram, the ensuing "contour plots" permit the selection of the optimum combination of time, temperature, and composition to attain a desired maximum hardness.

The compositional dependence of the minimum creep rate at constant temperature revealed a marked increase in creep strength at compositions just inside the two-phase boundary. This temperature and composition range corresponded closely to the area of retarded rate of age hardening noted in the contour plot of times to maximum hardness.

The effects of aging on the minimum creep rate of single-phase alloys were compared by means of the time-temperature parameters of Larson-Miller and Zener-Hollomon (as used by Dorn for creep correlations). The aged alloys were generally stronger, but at high stresses and low temperatures and at low stresses and high temperatures the

interpolated curve for single-phase alloys predicted a lower minimum creep rate than for two-phase alloys. The Larson-Miller and Z-parameters were shown to be equivalent functions.

INTRODUCTION

Despite the enormous volume of research that has been done on creep, no laws of a truly general and all-inclusive nature have been formulated. There is still need for work carried out on a wide range of simple materials, and their selection should be based primarily on the ability to reveal the basic factors. The deformational aspects of creep should be studied first separately from the effects attributable to precipitation hardening, and this has been done to some extent. However, regardless of the unsettled condition of creep theory today, an attack on the more complicated problem of creep during age hardening should be undertaken. In spite of the rather general recognition of this situation and the need for clarification, only a small amount of research has been directed specifically at this problem.

Since creep of commercial alloys generally occurs at elevated temperatures, the results are often complicated by transformations such as age hardening, tempering, resolution of one or more phases, and sometimes recrystallization. The transformations proceed with time independently of, or even enhanced by, the deformation accompanying the creep process. Any, or several, of these reactions may occur during creep, depending on the complexity of the alloy under consideration.

The present investigation has as its basic objective the investigation of the effects of age hardening on the creep behavior of polycrystalline aluminum-copper alloys. The effects of precipitation from solid solution on the creep properties of an alloy are generally such that the resistance to creep is increased. Precipitation hardening may occur when a solid solution, preserved by a rapid quench from a high temperature, undergoes precipitation from the supersaturated solid solution at some intermediate temperature. At appropriate temperatures, and in simple cases, as precipitation proceeds, the hardness and strength rise to maximum values and then diminish. Some alloys show a more complex behavior; for example, in aluminum-copper alloys, the composition of the precipitate, its nature, and its disposition within the matrix change during aging. It is not uncommon to find more than one maximum in the aging properties during the course of the reaction. However, in all precipitation-hardening processes, the hardness and strength ultimately decrease to a stable value, provided the temperature is not too low.

The tendency toward a maximum in the strength properties suggests that age hardening might be used profitably to enhance the creep properties of alloys. However, alloys possessing the maximum hardness before the creep test do not necessarily have the maximum creep resistance. Depending on the stresses involved and the temperature used, other structures may prove more stable. Considerations of the above nature reveal the importance of defining the initial state of the alloy. Here, the attention has been restricted to creep in alloys initially single phase. Then, one of the most important tasks is to separate the effects of age hardening on creep from the effects of creep on age hardening.

These two reciprocal effects are basic to an understanding of the problem of creep in age-hardenable alloys. In succeeding sections of the report, data are presented which should shed some measure of light on this extremely interesting aspect of creep. With sufficient information of this type, the behavior of age-hardenable aluminum-copper creep alloys can be deduced in general, and the conditions leading to optimum creep characteristics should be predictable.

This investigation was conducted at Battelle Memorial Institute under the sponsorship and with the financial assistance of the National Advisory Committee for Aeronautics. The authors wish to record a special note of thanks to Mr. R. D. Smith for his untiring efforts during the entire experimental program. The helpful discussions with Mr. R. L. Carlson are also gratefully acknowledged.

EQUIPMENT AND EXPERIMENTAL PROCEDURE

Preparation of Specimens

Four 25-pound ingots were prepared from 99.999-percent-pure copper and 99.996-percent-pure aluminum to compositions of 1, 2, 3, and 4 weight percent copper. Spectrographic and chemical analyses of the alloys are listed in table 1.

The melts were made in an old[1] clay graphite crucible using particular care to prevent the addition of extraneous material. The melts were stirred with a graphite rod to assure uniform distribution of the copper. They were then flushed with chlorine gas to remove hydrogen and to provide porosity-free ingots. The heats were poured into graphite-coated ingot molds and were water-cooled, giving pipeless ingots with dimensions of 2 by 6 by 18 inches.

After soaking for 2 hours at 850° F, the ingots were rolled to billets between $1\frac{1}{2}$ and $1\frac{3}{4}$ inches thick. After a homogenizing treatment

[1]To eliminate silicon pickup.

of 24 hours at 900° F, the billets were scalped to remove surface defects. Slabs were cut into 8-inch lengths for cross rolling to various thicknesses at a temperature of 850° F. The final reductions were made cold as indicated below:

Alloys, percent copper	Final cold reduction, percent
1	50
2	40
3	20
4	10

Final dimensions were a nominal 1/8 inch thick by about 9 inches wide, with strip lengths up to about 15 feet.

The specimens for creep testing were machined into tensile flats 7 inches long, 3/4 inch wide (at the shoulders), and 1/8 inch thick. The gage sections were 1/4 inch wide and $2\frac{1}{2}$ inches long. Small 1- by 1-inch blanks were cut from the same sheets for age-hardening runs. Afterwards, the creep specimens and the age-hardening samples were heat-treated at 540° C to an ASTM grain size of 1 ± 1, then water-quenched. All the creep specimens were electropolished in a glacial acetic acid and perchloric acid solution (100 to 30 parts by volume, respectively). Knoop indenter impressions were placed 2 inches apart on the gage section of the specimens and were used as gage marks during the creep runs.

When the specimens were not in use, either after the grain-size heat treatment or after the creep tests, they were stored in a refrigerator at -40° C. They were removed only when it was necessary to make other measurements, such as hardness readings and tensile tests.

Creep Measurements

All of the creep equipment was housed in a constant-temperature room in which the temperature was maintained at 26° ± 1° C. The creep unit was equipped with an electric resistance-type furnace, the power to which was controlled by a Variac connected to a Honeywell controller. The furnace temperature was controlled within ± 2° C, and the applied load was determined within 0.1 pound.

The creep runs were made in a specially designed furnace which permitted rapid heating or cooling of the specimen. A split-type, hinged, vertical-tube furnace was mounted on a horizontal track so that the specimen could be enclosed suddenly. Two narrow slit windows permitted visual observation of the specimens and the gage marks. Yoke and pin adaptors held the specimens at the shoulders.

A Gaertner microscope, which could focus at a distance up to 6 inches, was equipped with an internal illuminator. The magnification was 20X. The microscope was mounted on a vertical 4-inch micrometer slide with a sensitivity of about 50 microinches. The distance between the two gage marks was measured consecutively from outside the furnace. Since it took about 30 seconds to crank the microscope from one gage mark to the other, a stopwatch was used to record the actual time elapsed between readings.

Direct loading was utilized so that the load could be released quickly and the specimen quenched after a selected amount of creep. The weights were removed and a long cylindrical quenching tank was placed under the furnace. A pin holding the upper extension arm was pulled, and the counterbalanced creep specimen with the upper and lower extension arms would drop rapidly into water at 26° C.

The temperature variation along the length of the specimen amounted in some cases to about 2° C. An auxiliary heating coil was placed inside the furnace to permit finer control of the temperature gradient, and about 1/2° C spread was obtained. The time for the specimen grips to come within 5° C of the final temperature was less than 30 minutes, and, presumably, the reduced gage section of the specimen came to temperature in a shorter time. However, this could not be measured directly because of the necessity for quenching the specimen suddenly from the hot furnace.

X-Ray Technique

The X-ray examination given to the samples was of a simple type used previously in creep studies by Wood and Scrutton (ref. 1) and Wood and Rachinger (ref. 2). In this method, the X-ray beam impinged on the sample at normal incidence, and the diffraction pattern was recorded on a circular film in a "back-reflection" camera.

The photograms were taken using filtered cobalt radiation, which registered the $K\alpha_1$ and $K\alpha_2$ reflections of the (420) plane. The dispersion was high because of the long 10.0-centimeter sample-to-film distance. The diameter of the X-ray beam was about 0.5 millimeter, and the average diameter of the grains was 0.36 millimeter. Exposure times were 2 hours and more, depending on the diffuseness of the reflections.

Hardness Data

Hardness data were gathered from three sources - from the 1- by 1-inch blanks and from the shoulders and gage sections of the creep specimens. Vickers diamond-hardness numbers were obtained with a 10-kilogram load.

The blanks were aged in a salt pot at temperatures ranging from 200° to 400° ± 5° C. Samples were quenched periodically in water at room temperature at times estimated to give a fairly complete picture of the aging curves. At least five impressions were made on the ground surface, and the average value was used to plot the curves of hardness against time.

The hardnesses at the shoulders and gage sections of the creep specimens were obtained after the creep test. Some unevenness at the surface of the gage section resulted in distorted impressions, so an average diameter was used when necessary. Only three impressions were taken at the specimen shoulders, since the area of interest there was rather small.

Tensile Tests

The tensile tests were performed on the creep specimens after X-ray pictures and hardness values had been obtained. The spacing between gage marks and the distance between shoulder corners were determined before and after tensile testing. The dimensions of the cross section were also remeasured in the reduced portion of the crept specimen. All tests were run at a constant head speed of 0.0324 inch per minute and at a temperature of 26° ± 1° C. Since the lengths of the crept specimens varied, the strain rate varied between 0.00856 and 0.00708 per minute. The average value of 0.0078 per minute will be quoted hereafter.

The load was applied to a 9:1 lever arm by a suitably geared-down electric motor. The stress was determined from a calibrated ring gage (in conjunction with an SR-4 Baldwin strain indicator) linked in series between the lever arm and the moving cross head. The elongation was obtained by means of a dial gage mounted on the upper extension arm of the specimen. Yoke and pin adaptors held the specimens at the shoulders during the tensile test. The latter was usually discontinued shortly after the maximum load was detected.

Quantitative Metallography

The aluminum alloys containing 2 percent copper which were aged and crept at 400° C were selected for a detailed study of precipitation. The stress of 1,700 psi was chosen primarily because there were more creep data available at this level.

Here, as with the hardness measurements, three series of data were sought. Samples were cut from the unstressed blanks aged in the salt pot, from the stressed shoulders, and from the deformed gage sections of the same creep specimens. The specimens were mounted, polished, and

etched either with Keller's reagent or with a 1/2-percent solution of hydrofluoric acid. The entire polished surface was scanned under a magnification of 1,000X, and two to three representative pictures were taken of each sample (also at 1,000X). A fine grid consisting of 20 lines per inch was then superimposed on three copies of each photo, in three random orientations. The volume percent precipitate was determined by point counting (ref. 3) over an area of 3 by 4 inches on each print. An example is given below of the variation encountered by one observer in point counting two photomicrographs, each with three random grids superimposed, of an unstressed 2-percent-copper alloy aged at 400° C for 1 hour.

Photo	Grid position 1	Grid position 2	Grid position 3
1	80	76	66
2	124	118	122

A more limited check was made of the precipitation at 400° C in two 2-percent-copper creep specimens that were crept under a stress of about 1,270 psi. Since the precipitate was quite uniform, four photomicrographs were taken at random from each specimen with a magnification of 1,000X. Only two prints with random grid orientations were used here for each photograph, and 2- by 2-inch areas were selected for evaluation by point counting.

EXPERIMENTAL RESULTS AND THEIR EVALUATION

General Results

Since this investigation embraces several diverse topics, it probably would not be amiss to pause here for a brief survey of the entire experimental program.

Figure 1 has been constructed to show that portion of the aluminum-copper phase diagram which has been investigated during the past year. The phase boundary shown is that recommended in the "Metals Handbook" (ref. 4). Creep tests were made at those temperatures and compositions marked by circles. In general, the temperature dependence of creep has been obtained with the 2-percent-copper alloys, and the compositional dependence of creep has been determined at 300° C.

The locations of the age-hardening runs are denoted by the cross marks. Hardness data were obtained from all compositions at temperatures

between 200° and 400° C, whenever possible. Some mention has been made already of the creep tests, the hardness measurements, and the precipitation study. Reference to figure 2 may help to clarify the relationships among the separate sets of data.

As an example, consider the data obtained from aluminum alloys containing 2 percent copper aged at 400° C and crept under an initial creep stress of about 1,700 psi. First, the entire creep curve was determined. Several creep specimens were desired from various points along this creep curve (see fig. 2(a)). The additional specimens were obtained by testing at the same stress and temperature as before, but for successively shorter times. These specimens were quenched from the creep furnace at the indicated times in order to halt any further precipitation. This procedure yielded several specimens, representative of as many points along the creep curve, which were then measured for hardness, precipitation, and structural changes.

Figure 2(b) shows the curve of hardness versus time of the unstressed 2-percent-copper blanks aged in the salt pot at 400° C. The time dependency of the hardness of stressed 2-percent-copper alloys (i.e., the creep specimens) is also given. Two stressed age-hardening curves result because the hardnesses were measured at the shoulders of the creep specimens and also at the gage sections.

Figure 2(c) shows the locations on the creep specimens from which samples were taken for quantitative evaluation of the percent precipitation. The lowest curve depicts the course of precipitation in the same unstressed samples that yielded the age-hardening curve in figure 2(b).

It is hoped that figure 2 has clarified the interrelationships among the various data. A detailed consideration will now be given to all the data obtained during the course of this investigation.

Creep-Test Results

The compositions and temperatures at which creep tests were made have been indicated in figure 1. The initial creep stresses varied from 86 psi in a 2-percent-copper alloy tested at 540° C to 7,500 psi in the same alloy tested at 200° C. The test times were as short as 40 minutes and as long as 230 hours. A representative creep curve is presented by a logarithmic plot of total creep strain versus time in figure 3. Some creep curves deviated excessively from the average curve and were not used.

There is some spread among the creep curves belonging to the same stress and temperature group. The deviations are not believed to be

greater than those normally encountered, even in view of the unusual experimental requirements of this investigation. Some taper was detected in a few specimens because of hand grinding before electropolishing. The stresses for these specimens have been indicated as average values with appropriate limits. The basic information concerning the creep tests has been tabulated for more ready comprehension in table 2. It can be seen that the bulk of the work has been done with the 2-percent-copper alloys.

The shoulders and gage sections of the creep specimens were selected as likely spots to study the effects of strain on precipitation. It was hoped that the shoulders would be elastically strained and that the gage section would be plastically strained. A grid analysis was undertaken to determine the types of deformation occurring at these two sites. For this purpose a fine grid of 20 lines to the inch was applied photographically to some electropolished specimens. A 3-percent-copper alloy showed, after creep, an average strain of 0.901 percent in the gage section and 0.200 percent in the shoulder area. A 2-percent-copper alloy revealed the same strain in the shoulders as the first specimen, although the total creep strain differed by about a factor of 15. The pertinent details are compared below:

Specimen composition, weight percent copper	Creep test temperature, °C	Creep stress, psi	Duration of creep test, hr	Total creep strain, percent	Average strain at 26° C, percent, in -	
					Gage section	Shoulders
2	200	9,760	46	15	-----	0.200
3	200	8,000-[a]10,400	85	1.01	0.901	.200

[a]Step loaded.

The grid deteriorated at higher temperatures, so the amount of deformation during creep above 200° C was not determined. It appears from these data that the deformation at the shoulders is not elastic. Furthermore, it is possible that the strain at the shoulders does not change appreciably under similar stresses, even though the total creep strain may vary widely.

Several typical creep curves have been replotted in figure 4 with linear strain and time scales in order to illustrate the variations encountered under widely differing creep conditions. The 200° C curve is typical of the curves obtained at the lower temperatures and under relatively high stresses. The practically vertical curve obtained under a stress of 1,000 psi was concluded in about 40 minutes. The marker

movements were (relatively) so fast that stop watches were needed to time all measurements. Generally, however, other runs with such high creep rates were not attempted.

The two 1-percent-copper alloys of figure 4 were tested under almost identical conditions except for one important difference. In one case (the top curve), the specimen was allowed to come to temperature before the load was applied. This procedure was normally not possible except in the single-phase field, since it was desired to start age hardening concurrently with deformation. In the other case (the lower curve), the hot furnace was placed around the specimen at the same time the load was applied. The difference in experimental procedures, as reflected in the two creep curves, does not seem to give appreciably different results except at the very short times. The magnitude of this early difference, for all alloys, was usually much less than 1 percent strain, and this only at the shorter times.

The internal consistency of the creep data is indicated in figure 5, where the logarithm of the stress is plotted versus the logarithm of the minimum creep rate. These data points and extrapolated values are utilized later in the report, since the minimum creep rate is used as an index of the creep strength. The variation in the slopes of these lines with temperature approximates qualitatively the behavior observed in other creep studies (refs. 5 and 6).

An informative series of curves appears in figure 6 as a result of plotting minimum creep rates at 573° K against the composition. The data of Sherby and Dorn (ref. 7) were used to fill in the single-phase area, while the remaining two-phase data represent minimum creep rates of aging aluminum-copper alloys. The maximum rate of improvement in creep strengths occurs between 1 and 2 percent copper. Relatively little additional creep resistance is gained by increasing the copper content from 2 to 4 percent.

Low-magnification photomicrographs were taken of the surface deformation markings on aluminum-copper specimens crept to various strains. Figure 7 is arranged to show the compositional variation at 300° C (parts (b), (c), and (d)) and the temperature variation in 2-percent-copper alloys (parts (a), (c), and (e)). Extensive slipband formation, folds (ref. 8), and grain rotation is evident in the 1-percent-copper alloy, as well as marked upheavals at the grain boundaries and some grain growth. As the composition increases to 2 percent copper (at 300° C), the thickness of the slipbands decreases, but their density does not decrease to any noticeable extent. Some widening at the grain boundaries has occurred, and the folds are longer and narrower. The curved deformation markings at the grain boundary of the 3-percent-copper alloy reflect a greater strength of the matrix. The thin grain boundaries result from less grain-boundary sliding and are indicative of this alloy's enhanced creep resistance.

Proceeding from lower to higher temperatures in figure 7, first note the 2-percent-copper alloy crept at 200° C (fig. 7(e)). Fairly uniform slipbands have formed on these grains, while the folds are numerous and their surface upheaval is pronounced. Some grain-boundary fissures have formed (elsewhere) under this relatively high stress at a low temperature. The 2-percent-copper alloy stressed at 300° C shows a progressive increase in grain-boundary deformation and a relative decrease in slipband formation (fig. 7(c)). At 500° C very extensive grain-boundary migration and grain growth occurs (fig. 7(a)), which apparently is related to the viscous nature of the creep curve. From observations of the surface markings on these aluminum-copper alloys, it appears that the sequence of changes and the specific mechanisms of deformation are much the same as in creep of high-purity aluminum.

The question as to the actual grain size of specimens exhibiting extensive grain-boundary migration has been investigated in the 2-percent-copper alloy crept at 500° C under a stress of 201 psi. The grain size before creep was 2.8 grains per millimeter. Traces of the original grain boundaries can be seen on the as-crept surface in figure 8(a). After normal polishing and etching, the same area of the specimen was rephotographed and is shown in figure 8(b). The average grain size of the new surface was 1.06 grains per millimeter. An inspection of the grain-boundary traces in figure 8(a) reveals the strain-induced movement of curved boundaries toward their centers of curvature and the relatively restricted movement of the straight boundaries. The grain-boundary widening visible between the original grains in figure 8(a) does not appear in the large new central grain in figure 8(b). However, the highly disturbed regions immediately to the left and right of the large grain in figure 8(a) leave traces in figure 8(b) of smaller structures that have not merged completely with their new grains.

One more observation from the metallographic work deserves mention. The "light phenomenon" observed by Gayler in aluminum-copper alloys (ref. 9) has been a puzzling and controversial subject. This light-etching grain-boundary constituent occurs in aged alloys and has been considered (a) an integral part of the aging process (ref. 9), (b) a recrystallization process (ref. 10), and (c) a grain-boundary migration (ref. 11). Since these regions were rather small, even at magnifications of over 1,000X, they were difficult to find and to study. The application of stress to an aging 2-percent-copper alloy at 200° C has been found to give considerably widened and numerous bands of the "light phenomenon" at the grain boundaries. Furthermore, a reprecipitation has taken place within these regions under the accelerating influence of the applied stress. Additional evidence favoring the view of Polmear and Hardy (ref. 10) that this is a recrystallization process lies in the new orientation assumed by the precipitate in these regions.

A major goal of this investigation has been the determination and evaluation of the effects of age hardening on creep. The proposed procedure for accomplishing this goal is based on a comparison of the following two types of creep curves:

(1) The curves obtained when creep is accompanied by aging

(2) The curves obtained under identical circumstances but without aging

Obviously, both curves cannot be determined experimentally. Therefore, it was proposed to obtain high-temperature single-phase creep data which could then be extrapolated into the two-phase field. The latter data would be representative of creep without aging, while the corresponding creep-plus-aging curves could be obtained experimentally.

The value of such a comparison depends greatly on the accuracy of the extrapolated data. Numerous expressions involving stress, strain, time, creep rate, and/or temperature have been proposed (ref. 12). Here there should be an extrapolation capable of handling stress and temperature plus one other creep variable, such as strain or minimum creep rate. Theoretically, at least, if an equation includes temperature as a variable, then a temperature dependence for another variable should be forthcoming. However, the undue number of "constants" and their involved dependence on other factors mitigate against the use of expressions with three or more variables.

Two relatively simple functions have emerged lately which implicitly relate creep stress to the temperature and minimum creep rate (or to the temperature and time, in alternate forms). One of these functions, the so-called Larson-Miller parameter (ref. 13), is based on an equivalence of temperatures and minimum creep rates at any stress. The Larson-Miller parameter P takes the form

$$P = T(C - \log \dot{\epsilon}_s), \tag{1}$$

where T is the absolute temperature, $\dot{\epsilon}_s$ is the minimum creep rate, and C is a constant. The constant C is usually taken to equal 20, but other values may afford a better fit of the data. This parameter has been used extensively to relate and correlate both creep and tensile data. Although the exact shape of the plot of stress versus P is not specified, an extensive survey by Heimerl of many creep data (ref. 14) shows that the curve has a fairly well-defined shape. This finding gives increased confidence in evaluating the probable usefulness of an extrapolated curve.

Another implicit expression, which has led a more stormy existence, also relates the creep stress to a function of temperature and minimum creep rate. The expression has been championed recently by Sherby and Dorn for creep (ref. 7), although it was originally proposed for correlation of tensile properties by Zener and Hollomon (ref. 15). This function Z has the form

$$Z = \dot{\epsilon}_s e^{\Delta H/RT} \tag{2}$$

where ΔH is a constant, an experimental activation energy for creep which is closely akin to the activation energy for self-diffusion, and R is the gas constant. The other terms are as before: $\dot{\epsilon}_s$ is the minimum creep rate and T is the absolute temperature.

Both equations (1) and (2) have been used in an effort to compare the creep behavior of aging and nonaging aluminum alloys containing 2 percent copper. However, the actual value of the constants in each case has been calculated from the experimental data. Thus, the values of the constant C from equation (1) that were found to give the best fit to the creep data for the single-phase and two-phase alloys are 12 and 17, respectively. Similarly, the values 48,000 and 58,000 calories per mole of the constant ΔH were found to fit the data best in equation (2).

That these two constants should have different values is highly logical, because in one case there is creep in a solid solution undisturbed by aging effects, while, in the other case, aging exerts its complex influence on the creep process. Sherby, Orr, and Dorn were unable to correlate the creep data of age-hardenable alloys with ΔH for single-phase alloys (ref. 16), but this is understandable if a different process is controlling in aging alloys.

The experimental results are presented in figure 9 using the Larson-Miller parameter. The two curves for the 2-percent-copper alloys are representative of creep in unaged alloys (C = 12) and of creep in aging alloys (C = 17). The two points appearing at the highest stresses are obtained from the room-temperature tensile data for quenched single-phase and crept two-phase specimens. They help to delineate qualitatively the course of the curves at the high stresses, as does the curve for high-purity aluminum. The data for the high-purity-aluminum curve were obtained from the work of Sherby and Dorn (ref. 7) and that of Servi and Grant (ref. 5) (from the latter source at the temperature where grain-size effects were negligible). These two sets of data agree well with one another and with the value of 12 for C. Based on the shape of the high-purity curve, a smoothly bending line was drawn as the most probable curve for the single-phase 2-percent-copper alloys. On the other hand, the experimental data indicate a relatively sharp break in the curve for two-phase alloys.

The qualitative nature of the extrapolated portions of these curves precludes any quantitative calculations, but some trends can be predicted from figure 9. In general, the single-phase alloys are weaker[2] (i.e., have a higher minimum creep rate) over most of the stress range. At higher stresses, as the two curves tend to converge, the minimum creep rates become equal. Continuing to higher stresses, an inversion occurs and the single-phase alloys become stronger than the two-phase alloys.

At the higher temperatures, the two-phase alloys should overage quickly under stress, and the creep properties should approach those of an alloy initially overaged. This point was checked, as well as the possibility that another inversion in creep strengths might occur at the higher temperatures (lower stresses). A specimen was overaged by heating for 4 days at 300° C and then was crept under a stress of 2,400 psi at 300° C. The change in position because of prior overaging is indicated by the arrow in figure 9. At an assigned temperature of 500° K the minimum creep rates of the overaged alloy and of the single-phase alloy are approximately equal. The large, coalesced particles in the overaged alloy apparently contribute little toward strengthening the matrix.

At even higher temperatures single-phase alloys should become stronger. This behavior has been reported by Russian workers. A slight convergence of the two-phase and single-phase curves can be noted as the stresses decrease (below 1,700 psi) or as the temperature increases. A trend of this type implies an inversion in relative strengths similar to that already noted at the higher stress levels. To illustrate the effect of even this slight convergence, minimum creep rates have been calculated for stresses between 800 and 1,700 psi and are plotted in figure 10. Figure 10(a) shows this inversion in minimum creep rates as the temperature increases, while in figure 10(b) the same result is obtained with decreasing stresses.

The same data used in figure 9 were also plotted against the Z-parameter of equation (2). The resulting curves appeared to differ markedly from those shown in figure 9. Actually, however, the calculated results are the same because the Larson-Miller parameter and the

---

[2] When $\left(P_{C=17}\right) - \left(P_{C=12}\right) > 5T$, where P is the Larson-Miller parameter with the indicated value of C and T is the absolute temperature. The meaning of this inequality can be understood readily in the case of a constant temperature. Then, $5T$ is also constant and is equivalent to a constant distance on the parameter scale. As the two curves diverge more or converge less than this distance, the minimum creep rate for the single-phase alloy becomes more or less, respectively, than that for the two-phase alloy.

Z-parameter are equivalent functions. This is shown readily by recasting the Larson-Miller parameter to the same form as the logarithmic Z-parameter. That is, by solving equation (1) for C,

$$C = \log \dot{\epsilon}_s + (P/T) \tag{3}$$

and by taking logarithms of equation (2)

$$\log (Z) = \log \dot{\epsilon}_s + (\Delta H/2.3RT) \tag{4}$$

It is obvious that C corresponds to log Z and P corresponds to $\Delta H/2.3R$. Oddly enough, there has been a wide acceptance of the Larson-Miller parameter with the constant equal to 20 but a wide split of opinion as to the constancy of ΔH.

The variation of ΔH with stress has been investigated by several methods and some dependency was evident. However, since the data were neither too plentiful nor definitive, and since the ΔH's calculated by equivalent methods conflicted somewhat, a single value was used over the entire stress range. That the ΔH's used were adequate to correlate all the experimental data is attested to by the good fit to the curves.

An interesting sidelight of these parameter plots is that they permit an activation energy to be calculated from data obtained at only one temperature. If it is established that the experimental parameter-plot curve is valid, then any selected point along the curve can yield any number of minimum creep rates and corresponding temperatures. A simple calculation of ΔH's at 2,400 psi versus composition of aluminum-copper alloys indicated an increase in ΔH from 32,000 to 56,000 calories per mole for from 0 to 4 percent copper.

Age-Hardening Curves

The temperature-composition locations on the phase diagram where the alloys were age hardened are given in figure 1. The duration of the tests varied between 110 minutes and 7 days, and the temperature range extended from 200° to 400° C.

The age-hardening curves for the alloys with 2 percent copper are presented in figure 11. Some scatter in the hardness points is evident, but not more than is generally found in the literature (refs. 17 and 18). It will be noticed that the estimated times to maximum hardness have been indicated by small arrows in figure 11. The times decrease with

increasing temperature, but the trend is reversed between 300° and 400° C. The maximum hardness also appears to follow the same pattern. These apparently inconsistent data will be rationalized later on the basis of a kinetic analysis of the age-hardening process.

The average hardnesses of several quenched specimens are plotted versus composition in figure 12. The values of the present investigation are compared with those from other investigations (refs. 17 and 18) and are seen to lie well above the other data. However, it was noticed that the quenching temperatures differed somewhat. This factor may account for the apparent discrepancy in results. The more important age-hardening data are tabulated for easy reference in table 3.

Hardness data were also obtained from the creep specimens, both in the gage section and at the shoulders. It was necessary to take the measurements before tensile testing because the hardness numbers were considerably higher after the additional room-temperature deformation. The hardnesses of the stressed alloys are included in the tabulation of creep data in table 4. The hardness values obtained here fell into two groups when compared with the maximum hardness of the corresponding unstressed alloys. That is, one group of hardness curves was obtained close to maximum hardness (see fig. 13(a)), while the other group fell well past this point (see fig. 13(b)).

In figure 13(a), the hardness curve for unstressed 2-percent-copper alloys aged at 400° C is compared with the hardnesses from crept alloys of the same composition. The hardnesses of the alloys stressed at 1,700 psi hint at the presence of two maximums. The gage-section data seem to be descending from a very early maximum, while the shoulder hardnesses show a definite peak at a later time. The opposite trend is noted for stresses of 1,235 and 790 psi. For these latter stresses it appears that the shoulder hardnesses have reached their maximums before the gage-section hardnesses, although additional data for earlier times would be needed to verify this point.

The contradictory nature of these results can be resolved readily if the hardnesses are considered not in relation to the time of stressing, but rather in relation to the total creep strain. This comparison is made in figure 14 by plotting the three shoulder-hardness curves of figure 13(a) versus time (fig. 14(a)) and then again versus total creep strain (fig. 14(b)). Two radically different groups of curves result. In figure 14(a) there is no obvious relationship between stress, time, or hardness. However, in figure 14(b) three distinct curves have sorted themselves out of the same data. The hardness levels decrease directly with the stress, while a hardness peak appears at essentially the same total creep strain of about 1.4 percent. Furthermore, through a fortuitous scatter in the individual creep curves, it can be seen that the

contribution of time to the hardness (after maximum hardness) is negligible compared with that of the strain.

A similar plot of the gage-section hardnesses versus total creep strain reveals qualitatively the same behavior, but apparently the more inhomogeneous deformation in the gage sections is responsible for a little scatter in the hardness values. Also, the general hardness level here lies slightly below that of the shoulders. This is probably due to the more rapid aging in the gage sections. These data will be considered in more detail later in connection with the discussion of the tensile data.

A break was drawn in figure 13(a) in the latter part of the hardness curves for specimens stressed at 1,700 psi. This liberty was taken on the basis of the findings presented in figure 13(b). The curves in figure 13(b) represent the second group of hardness data obtained from stressed specimens. The hardness of unstressed 2-percent-copper alloys aged at 300° C is compared with the hardnesses obtained from specimens crept under stresses from 2,400 to 1,700 psi at 300° C. For each stress, there is a sudden drop in the curve of hardness versus time, and the "transition" times increase with decreasing stress. Reference to the creep curves of the specimens from which the hardnesses were obtained reveals that the hardness breaks occur during tertiary creep. This relationship is portrayed in figure 15 where the hardness data of figure 13(b) are superimposed on representative creep curves.

In general, the lower hardness readings were obtained from ruptured specimens (well back from the point of rupture). The microstructure in the gage section of a ruptured 2-percent-copper specimen is shown in figure 16. Here, as in the work of Sully and Hardy (ref. 19), shear displacements can be seen across boundaries favorably oriented to the applied stress, as well as grain-boundary fissures transverse to the stress direction. It would seem that the lower hardness values obtained here are associated with the presence of these fissures. This point could best be clarified, however, by a similar series of hardness measurements on specimens from tertiary-stage compressive creep.

Recourse to an alternate plot of hardness versus total creep strain reveals that the hardness falls off gradually and smoothly with increasing strain. Wilm's observations (ref. 20) are consistent with this finding. His X-ray investigation of aluminum during tertiary creep showed no radical change in the mechanism of deformation that characterized the secondary stage of creep. The subgranular structural condition was present almost until fracture. The apparent abruptness of the drop in the hardness versus time plots is undoubtedly a reflection of the accelerated elongation occurring in a relatively short time.

Precipitation Data

A deceptively small amount of quantitative precipitation data resulted from a rather disproportionate amount of labor. Furthermore, it was deemed advisable to label the results "relative" rather than absolute. This qualification is applied because of the well-known difficulties stemming from work with small amounts of fine particles at high magnifications. The selection of a limited number of samples to represent the total structure is a critical aspect of the problem. Operator judgment in deciding whether a grid intersection touches a particle is an important factor in point counting. Perhaps the greatest source of inaccuracy lies in overetching the polished sample, since this could easily make particles of the size treated here appear twice their actual diameter. However, inaccuracies from this source were held to a minimum, so there is a reasonable degree of confidence in the results.

The bulk of the effort may be summed up in two diagrams shown in figure 17. Figure 17(a) gives both the relative amounts of precipitate appearing during reaction at 400° C in unstressed 2-percent-copper alloys and the hardnesses of the same samples. A parallel comparison is made in figure 17(b) for stressed 2-percent-copper alloys from the shoulders and gage sections of the creep specimens.

Although some precipitate is evident in the unstressed alloys before the hardness maximum is reached, it is mostly at the grain boundary. The shoulder alloys, however, show over 4 percent precipitate, mostly in the matrix, at maximum hardness. A rough estimate of the times required to reach 50 percent of the total precipitation follows:

	Aged at 400° C; unstressed	Stressed at 1,700 psi at 400° C	
		Shoulders of creep specimens	Gage sections of creep specimens
Precipitation half-times of 2-percent-copper alloys, min	75	43	26

These half-times are consistent with the hardness levels of the three hardness curves. The unstressed hardnesses are generally higher than those from the shoulders, and the shoulder hardnesses are slightly above those of the gage sections. This is what one would expect beyond maximum hardness, since the alloys that reacted fastest would overage (be softer) sooner than the more sluggish alloys. Not only does the gage-section precipitation occur faster than that at the shoulders, but also the maximum amount seems to be less. This behavior conforms to that of a strain-sensitive precipitation process, in which the amount of intermediate precipitate also depends on time. Ostensibly the accelerated

reaction under the greater strain rate in the gage sections inhibits the formation of the maximum possible amount of precipitate. On the other hand, the relatively low strain rate in the shoulders permits the reaction to proceed to a greater extent.

Three series of photomicrographs representing the three precipitation curves are displayed in figures 18 and 19. Figure 18 shows precipitation in the unstressed 2-percent-copper alloys aged at 400° C. The precipitate is relatively large, widely spaced, and coalesced into more or less spherical particles of $CuAl_2$ (or θ). A few sharp particles of the intermediate precipitate θ' indicate the extent to which equilibrium conditions have been attained. Actually, θ' is quite persistent and is probably present in appreciable amounts.

Figure 19(a) shows precipitation in the same alloys at the same temperature, but under the stress conditions prevailing at the shoulders of the creep specimens. The finer, more dispersed, and more numerous precipitate particles in this series are immediately seen. The growth in thickness and diameter of the Widmanstätten plates is also evident as the time increases. It is believed that the platelike particles are θ' from their similarity to published photomicrographs of θ' (refs. 10, 18, and 21) and from the metastable solubility curves for θ' (refs. 22 to 24).

Figure 19(b), showing precipitation in the gage sections of the creep specimens, is similar to figure 19(a). If anything, the θ' particles appear smaller and more numerous in figure 19(b). There is more precipitation, however, only up to about 70 minutes.

The success of the total creep strain as a parameter for rationalizing the hardness data of stressed alloys prompted a similar plot of precipitation versus total creep strain. The available data are plotted in figure 20 and show little difference from the corresponding curve of precipitation versus time (fig. 17(b)). This situation arises simply because, in this particular case, the total creep strain in the specimens stressed at 1,700 psi varied directly with the time of the test. (Different hardness curves were obtained previously with the two variables, time and strain, because of experimental scatter in the creep curves of specimens stressed at 1,235 and 790 psi.)

To determine whether the relative amount of precipitation was influenced primarily by time or by total creep strain, two specimens with practically the same time but widely differing creep strains were studied. The details of testing at 400° C and the results of point counting are presented on the following page:

Specimen composition, weight percent copper	Testing time, min	Creep stress, psi	Total creep strain, percent	Relative amount of precipitation in gage section, percent
2	202	1,220	5.9	6.13
2	199	1,290	20.0	5.50

From the constancy of the time, percent precipitation, and stress (average stress, 1,260 ± 3 percent), it appears that total strain is not too sensitive a parameter for these overaged alloys. It was concluded previously that a greater strain rate tended to decrease the maximum amount of intermediate precipitation. These data also indicate less precipitation for the higher strain rate. If the two data points from the table are now compared with the gage-section precipitation curve in figure 20, it is seen that the amount of precipitation is greater under the higher stress. The overall picture is resolved simply by considering the data with regard to the three variables, time, strain, and percent precipitation. A three-dimensional plot reveals that a maximum in precipitation occurs not only with time but also with strain. The precipitation in the shoulders occurs at some low, essentially constant strain and gives the three-dimensional precipitation peak. The unstressed precipitation curve and the gage-section precipitation curve have less precipitation and fall at lower and higher strains, respectively, than the shoulder precipitation curve. The two data points from the table have less precipitation and fall past the maximum in point of time. The concept of a critical strain resulting in greatly increased property changes is not new and appears to apply here with equal force.

Even if the total (initial) precipitation were directly related to the applied stress, it would be difficult to reconcile the amount of precipitation measured here with that demanded by the phase diagram. A 2-percent-copper alloy in equilibrium at 400° C should have about 0.61 volume percent $CuAl_2$ in a matrix of α solid solution. If the precipitate were entirely θ', the total would reach about only 0.64 percent (figure based on Hardy's unit cell (ref. 25)). The maximum amounts of precipitation measured in the 2-percent-copper alloys aged at 400° C are recapitulated below for convenience:

	Unstressed alloy	Shoulders of creep specimens	Gage sections of creep specimens	
		Stress = 1,700 psi	Stress = 1,220 psi	Stress = 1,700 psi
Maximum measured precipitation, volume percent	3.53	10.75	6.13	8.27

The possible sources of error in these measurements have been enumerated at the beginning of this section. If a 50-percent error were assumed, there would still be a wide gap between the theoretical amount and the measured amount of precipitation.

Although reports from many reliable sources have contained evidence of unusually high amounts of precipitation, this fact has not received much attention. Polmear and Hardy published electron microscope pictures of θ' in an aluminum alloy containing 4 percent copper aged at 190° C (ref. 10). The magnification was 20,000X. A rough estimate of the amount of precipitation in the 96-day picture was obtained by point counting and gave about 13 percent. The equilibrium amount of θ is about 4.6 volume percent. The "typical microstructures" published by Shaw, Shepard, Starr, and Dorn (ref. 26) for alloys of aluminum with 3, 4, and 5 percent copper should possess 3.2, 4.5, and 5.9 volume percent $CuAl_2$, respectively. A visual estimation of the precipitation in these photomicrographs exceeds these figures by a wide margin. Guinier (ref. 27) quotes a figure of 9 volume percent θ' if all the copper in an aluminum alloy containing 4 percent copper is precipitated at 200° C. It was shown recently, in a quantitative study, that the percent precipitation in magnesium-aluminum alloys was increased by creep stress (ref. 28).

Quantitative measurements of θ' have been made by X-ray methods (refs. 25, 27, and 29). The quantity of θ' present is obtained as a percentage of the total possible amount by intensity comparisons of appropriate θ' reflections. Hardy, Silcock, and Heal reported that the absolute intensity of the θ' spots was greater than that calculated by assuming all the copper to be present as θ' (ref. 25). It would be interesting to learn how much precipitation is predicted from the absolute intensities. Some consideration has been given to compositions other than $33\frac{1}{3}$ atomic percent copper in the θ' unit cell, but none of these attempts has yielded a better fit with the observed intensities of θ' diffractions than that obtained by Preston (ref. 30).

The possibility that the initial θ' may have less copper than the stoichiometric composition of $CuAl_2$ is very attractive. Reference to the hypothetical free-energy composition diagram in figure 21 shows that a larger amount of initial precipitation is possible if the solute concentration is less. The compositions of the equilibrium phases (α and θ) are determined by the points of tangency of the common line. However, if the initial precipitate has the dashed free-energy curve, then its composition will correspond to A, while that of α changes very little. The lever law predicts an increase in the weight fraction of precipitate depending on the extent of the shift from θ to A. Therefore, the anomalously high percentages of precipitation reported here can be rationalized simply by postulating an initial precipitate with a copper content less than that in $CuAl_2$.

This is not a new idea. The theoretical aspects of an initial precipitate possessing other than the equilibrium composition have been considered by Dehlinger (ref. 31), Scheil (refs. 32 and 33), and Masing and Nickel (ref. 34). Evidence amenable to interpretation on the basis postulated has been obtained experimentally by Gerlach (ref. 35) and Underwood (ref. 36) with gold-nickel alloys and by Gayler (ref. 9) and Saulnier (ref. 37) with aluminum alloys containing 4 percent copper.

Dilatation measurements of Kempf and Hopkins (ref. 38) during aging of an aluminum alloy containing 6 percent copper exhibited anomalous initial increases in length. A contraction should occur if the precipitate is the dense $CuAl_2$. Brick and Smith in their discussion (ref. 38) demonstrated that the expansion could be explained if part of the precipitate were assumed to have the newly announced θ' structure of Wassermann and Weerts. The dilatation data have been reinterpreted by assuming that it is not an unknown amount of θ' causing the expansion but an "initial" precipitate of unknown composition.

The density of the alloy was calculated at two temperatures from the measured maximum changes in length (ref. 38). This gave two expressions relating the specific volume of the alloy to the specific volumes of the assumed phases (α solid solution and the initial precipitate). The two unknowns, the composition and the density of the initial precipitate, were then obtained by simultaneous solution of the two equations. This procedure gave the composition of the initial phase to be about 6.8 percent copper at 400° C and its density to be about 2.82 grams per cubic centimeter. On the basis of these data, a 2-percent-copper alloy aged at 400° C should possess about 9.3 volume percent initial precipitate.

The coincidence of this value with the precipitation data is indeed startling when one considers the oversimplification inherent in the assumptions and the roughness of the calculations. Moreover, the way in which the precipitation, metallographic, X-ray, and dilatation data fall together leads one to believe that a more refined experimental investigation of this problem would be justified. Certainly, the present theories of precipitation in metallic solid solutions should be reexamined. If the initial precipitation actually does exceed the equilibrium amount, then there should be an eventual decrease. The precipitation curves in figure 20 show such a decrease with the gage-section data.

Tensile-Test Results

It was felt that the additional data forthcoming from tensile tests of crept specimens would provide worthwhile auxiliary information on the creep process. Tensile data were obtained with a constant head speed of 0.0324 inch per minute, or a strain rate of about 0.0078 per minute.

The ultimate tensile strengths for the precrept specimens are tabulated in table 4 with the creep data.

Tensile tests were performed on only those creep specimens that (a) had not gone to rupture, (b) did not exhibit undue taper, and (c) had deformed homogeneously during creep. Nevertheless, since emphasis was placed primarily on obtaining the creep data, the condition of the specimens for tensile testing was given secondary priority. For example, surface upheavals of the grains and grain-boundary shear resulting from high-temperature creep left roughened surfaces, grain growth at the higher creep temperatures introduced a new variable, the creep elongations presented different gage lengths for the tensile tests, and so forth. All in all, however, it is believed that the tensile tests give a qualitatively correct picture of the actual behavior.

The problem arose of determining the effective gage lengths of the crept specimens. The overall elongation was measured from shoulder to shoulder during the tensile test, but the cross-sectional area varied over the filleted portions of the specimen. In preference to using the inexact, but more convenient, measured shoulder-to-shoulder distance for calculating the strains, an alternate method was devised for obtaining an "effective" initial gage length. The details are presented in appendix A.

A typical series of stress-strain curves is presented in figure 22(a). The 2-percent-copper alloys were crept at a stress of 790 psi at 400° C to the strains indicated in the table and were then tensile tested at room temperature. In an effort to visualize the part played by prior creep strain on the tensile properties, the flow stress at a strain of 4 percent, obtained as indicated in figure 22(a), was plotted versus the precreep strain in figure 22(b). The tensile flow stress for a creep strain of zero was obtained with a single-phase specimen quenched from 540° C. The flow stress decreased quickly with increasing creep strain and then began to rise gradually at about 3 percent strain. In general, this is the behavior observed in all the specimens from which data were obtained. An exception to the rule was noted for the 2-percent-copper alloys crept at a low temperature (200° C) and under a high stress (e.g., 6,000 psi). Under these conditions, the tensile flow stress decreased at about the same rate as in the other alloys, but only after reaching a value greater than that of the alloy with zero precreep. A difference in recovery characteristics is probably operative in the latter case.

The effect of composition on the tensile flow stress of the aluminum-copper alloys crept at 300° C is depicted in figure 23. The data were obtained from curves such as that in figure 22(b) by plotting the flow stress at a creep strain of 1 percent against the composition. The

limited amount of data falls into three fairly well separated groups, according to the original creep stress. The increase in tensile flow stress is roughly equal to the difference between the creep stresses.

Figure 24 reveals the effect of creep stress on the tensile flow stress of the 2-percent-copper alloys crept at 300° and 400° C. The flow stresses were again obtained from curves such as that in figure 22(b), but for a creep strain of 2 percent. The effect of prior creep stress on the tensile flow stress at 400° C is slight, but becomes appreciable at 300° C. The scanty data available for 200° C suggest an even more pronounced effect - the increase in tensile strength is about double the increase in creep stress. Sherby and Dorn (ref. 39), among others, have shown that, under constant stress, a constant substructure results at equal creep strains, regardless of the temperature. A different (constant) substructure is obtained at a different creep stress. Since the tensile comparisons are made here at the same creep strain, it follows that the observed effects are attributable primarily to the substructures inherited from the creep stresses.

The relation between curves of hardness and flow stress and those of the prior creep strain in 2-percent-copper alloys is shown in figure 25. The two sets of curves purport to distinguish between high-temperature (and low stress) behavior and that at low temperature (and high stress). The additional effects of age hardening are superimposed on the overall results. The hardness and flow stress at zero precreep strain are not known exactly, since values are known only for alloys quenched from 540° C. Here, the values for single-phase alloys quenched from 200° and 400° C would be helpful but are patently impossible to obtain. The hardnesses for zero precreep strain were obtained by extrapolation of the 200° and 400° C unstressed hardness curves to zero times.

There are marked qualitative differences between the two sets of data. The alloys crept at 7,500 psi and 200° C appear to have a direct correspondence between the tensile and hardness curves. Recovery would be expected to play a relatively unimportant role at this temperature. The hardness and tensile data for a creep stress of 1,700 psi and temperature of 400° C do not exhibit any correspondence with one another at the early strains; however, a level value is reached in each case after a creep strain of about 3 percent. At this temperature relatively rapid recovery would be expected. The slight peak in hardness at an early strain corresponds to a rapid decrease in the tensile flow stress. The latter curve bears a striking resemblance to those established by Sherby, Goldberg, and Dorn (ref. 40) with prestrained, crept, and tensile-tested high-purity aluminum.

The evidence is fragmentary, yet it points to the dual nature of the hardness data - the contribution to hardness of the age-hardening process and the contribution to hardness of the structural deformation.

The tensile data, on the other hand, appear to react primarily to the deformational characteristics of the metal structure. On this basis, the data are explicable. The hardness peak at 400° C is due to the age-hardening component of hardness in the recovered structure. The drop in the corresponding tensile curve reflects the progressive recovery of the deformed crystal structure. The 200° C data, on the other hand, run identical courses, presumably because recovery has not operated to any great extent.

X-Ray Photographs

The X-ray technique used in this investigation is capable of revealing the effects of deformation in the crystalline lattice. Valuable corroboratory information on the nature of the deformation process may be deduced from the appearance and distribution of the spots on the film. The results of the X-ray investigation of the 2-percent-copper alloys crept at 1,700 psi and 400° C are summarized in table 5. The X-ray photographs are reproduced in figure 26.

The first sample was aged but not stressed and shows strong sharp-spot reflections originating in the matrix. Several of the sharp spots also have very diffuse weaker reflections fanning out from them on one side. These diffuse reflections probably result from some residual θ' precipitation, since the pattern of the matrix is usually less sensitive to alterations than is that of the precipitate. The hardness and precipitation curves both indicate that 1,470 minutes is well past the point of maximum hardness, but the photomicrograph taken after 960 minutes (fig. 18) still reveals a few sharp, platelike particles.

The sample strained 0.80 percent shows a slight distortion of the matrix, since the size of the sharp spots approaches 2 millimeters, as compared with sharp spots of 1.2 millimeters or less from the unstrained sample. At 1.29 percent strain the spots become more diffuse and spread out to about 3 millimeters. At 2.89 percent strain, the process continues, and the spots reach a size of 6 millimeters. At this stage of deformation and aging, the grains are probably undergoing distortion of some sort (fragmentation and/or bending). The diffuse streaking may also be due in some measure to the rearrangement of atoms during aging.

At 7.58 percent strain, discrete spots are no longer observed. Instead, there are arcs 10 to 15 millimeters long on the Debye rings. The arcs have a wealth of fine structure, that is, distinct diffraction spots, which are indicative of polygonization. At 33 percent strain, the arcs are still more continuous and the detail in the fine structure is still finer. The long arcs reveal the extensive disorientation between the subgrains, and the individual sharp diffraction spots represent the individual subgrains. With both the 7.58 and 33 percent

strains, some unresolved reflections occur outside the range of the alpha solid-solution 420 circles. These are probably due to the θ' phase, because at this stage the photomicrographs indicate extensive platelike precipitation.

It is clear that under creep strain the matrix grains are broken up by rotation of portions of the grains. After large creep strains of 7.58 and 33 percent, the grains are broken up into many fine discrete domains. In the samples with lesser amounts of strain it could not be determined, from the techniques used, whether the grains were broken up into discrete domains or were merely bent.

The stationary technique used here reveals, in a qualitative manner, the structural changes taking place during creep in the age-hardening alloys. More refined X-ray measurements will depend on more elaborate equipment and procedures. From the limited study that has been made here, it seems likely that the deformational process proceeds in much the same sequence as that observed in pure aluminum (ref. 40). However, when comparisons with pure aluminum are made at equal strains, it appears that the structural changes are accelerated in the age-hardenable alloys.

Kinetic Analysis

This investigation has uncovered several interesting aspects of age hardening that are concerned more with the kinetics of the process than with the interrelationship with creep. However, since the results lend themselves to a better understanding of age hardening without stress, it is conceivable that a study of age hardening under stress would profit similarly.

The basic data are contained in table 3. A plot of logarithmic time to maximum hardness versus the reciprocal of the absolute temperature yielded no systematic trends with either composition, slopes, or intercepts. In fact, straight lines were not obtained. This latter fact is understandable, however, because, at higher and higher age-hardening temperatures, the rate of a reaction passes through a maximum and then becomes progressively slower as the equilibrium phase boundary is approached.

Therefore, the logarithmic time to maximum hardness was plotted against the ratio of T_r/T_s, where T_r is the absolute temperature of the age-hardening reaction and T_s is the absolute temperature of the $\alpha:(\alpha + \theta)$ solvus for the particular composition under consideration. This procedure, in effect, normalizes the (different) temperature scales for each alloy so they may be compared with one another. Now, T_r/T_s approaches 1 for each alloy as the reaction temperature approaches the

solvus temperature. A plot of the appropriate data from table 3 appears as in figure 27. The four curves are arranged in order of composition, with the 4-percent-copper alloy showing the fastest reaction (i.e., the shortest time) to maximum hardness. The other curves rise systematically, and all minimums appear to fall near a T_r/T_s value of 0.9. One advantage of this type of plot is that all four curves must rise to infinite times at $T_r/T_s = 1$. This characteristic permits one to draw the probable course of the curves with only a relatively few experimental points.

In order to visualize more readily the relative rates of age hardening over a range of compositions and temperatures, these data have been replotted on the aluminum-copper equilibrium diagram. In figure 28 lines of constant time to maximum hardness have been superimposed on the two-phase field. The dashed line, roughly paralleling the phase boundary, represents the curve of maximum rate of age hardening. This curve was obtained from the four minimums appearing in figure 27. Slight bulges, representing a retardation of aging rates, are apparent in the constant-rate contours at about 2 percent copper. These unexplained deviations seem to be a real effect (ref. 36), possibly connected with the thermodynamics of the system. It is of more than passing interest to note that the maximum gain in creep strength at 300° C is obtained near this composition.

The significance of the curve of maximum rate of age hardening may be seen by following some composition line upwards (to higher temperatures). At the low temperatures the rates are slow (i.e., the times are long), but as the temperature increases the rate correspondingly becomes faster. However, after passing the curve of maximum rate of age hardening, the times begin to increase and presumably go to infinity as the equilibrium phase boundary is approached.

Knowing the temperatures at which the maximum rate of age hardening occurs, one can now explain the apparently irrational behavior of the maximum hardness values with temperature. If the maximum hardnesses (from table 3) are plotted for each alloy versus their respective reaction temperatures, it will be seen that some hardness curves have a minimum at higher temperatures. These minimums coincide closely with the temperature corresponding to the maximum rate of age hardening. The maximum-hardness curves in this report do not define the minimum for all compositions because of insufficient data. However, Gayler's extensive investigation of aging in a 4-percent-copper alloy (ref. 18) shows the hardness minimum clearly (when her high-temperature curves are reinterpreted to conform with the experimental data). Also, Swindells' and Sykes' curve of hardness versus temperature for a slowly heated aluminum alloy containing 4.8 percent copper (ref. 23) depicts the minimum plainly at about 420° C. These combined results suggest that the maximum hardness for an alloy aged at various temperatures is least when attained in the shortest time.

The smoothed maximum-hardness data from this investigation (at the higher temperatures) and from Hardy's (ref. 17) (at the lower temperatures) have been incorporated into the contour plot shown in figure 29. Here, the lines of constant maximum hardness have been superimposed on the aluminum-copper equilibrium diagram. The curve of maximum rate of age hardening was obtained from figure 28. Hardness values were assigned to the phase boundary from the measurements on alloys quenched from 540° C. (If the hardness of alloys quenched from the phase-boundary temperature is less than the 540° C hardness, the indicated phase-boundary points would be shifted somewhat toward higher copper concentrations.)

An inspection of the maximum-hardness contours as one goes to higher temperatures along a line of constant composition is informative. The hardnesses fall rapidly at first, then more slowly until the curve of maximum rate of age hardening is reached. The maximum hardnesses then rise slightly and fall off again as the single-phase region is approached.

The value of a diagram of this nature lies in its portrayal of the gamut of age-hardening possibilities over a wide range of compositions and temperatures. In connection with the "kinetic" contour plot of figure 28, the selection of the optimum combination of alloy composition, time, and temperature to attain a desired hardness can be ascertained readily. If sufficient time were available, it would be interesting to trace the destination of the higher-hardness contours at the lower temperatures. They must double back ultimately, unless pure aluminum is capable of attaining comparable hardnesses at very low temperatures.

CONCLUSIONS

Effects of Creep on Aging in Aluminum-Copper Alloys

The effects of creep stress (and/or strain) on the aging process were established by quantitative evaluation of the percent precipitation, and by hardness, X-ray, and tensile testing. The following results and conclusions were obtained from this phase of the investigation:

1. The amount of precipitation induced by aging during creep was two to three times greater than that occurring in unstressed alloys, depending on the magnitude of the strain. The maximum measured amount of precipitation was about 10 times greater than that calculated from the phase diagram, assuming the equilibrium precipitate. This behavior was confirmed qualitatively by other investigators. From considerations of the pertinent X-ray data, of various investigations of precipitation in aluminum-copper alloys, and of measurements on other aging alloys, it was concluded that a precipitate composition less than that generally assumed would best explain the observed behavior. From published dilatation measurements, a simplified calculation was made of the amount of

"initial" precipitation expected on the basis of a nonequilibrium composition. The result of this calculation agreed closely with the measured maximum amount of precipitation.

2. In order to explain the interrelationship between stress and precipitation, it was necessary to resort to a three-dimensional plot of time versus creep strain versus percent precipitation. A maximum in the stress-induced precipitation surface was found to be a function of the creep strain as well as of the aging time.

3. Hardness changes during aging under stress suggested that the time to maximum hardness was decreased by increased strain. When the stressed-hardness values were plotted against creep strain, and not aging times, a direct dependence of hardness level on creep stress ensued.

4. Hardness measurements on unstressed alloys yielded "contour plots" of constant time-to-maximum-hardness curves, which, when superimposed on the phase diagram, revealed the temperature-composition course of the curve of maximum rate of age hardening. A similar contour plot of constant-maximum-hardness curves, when used in conjunction with the above kinetic contour plot, is capable of divulging the optimum combination of time, temperature, and composition to attain a desired maximum hardness.

5. X-ray photograms suggested that the same sequence of deformational changes occurs in aging and crept aluminum-copper alloys as occurs in pure crept aluminum. Furthermore, the process seems to be accelerated somewhat in the alloys.

6. The tensile flow stress of crept specimens decreased with increasing creep strain up to about 3 percent, then rose gradually thereafter. The flow stress at a constant creep strain varied directly with composition, and an increase in creep stress raised the flow stress by about the same amount. The dual nature of the hardness measurements could be explained by assuming separate deformational and age-hardening contributions to the hardness; on the other hand, the tensile flow stresses appeared to be dependent on the deformational condition only of the crept specimen.

Effects of Aging on Creep in Aluminum-Copper Alloys

Aging in quenched alloys was initiated simultaneously with the application of the load, and different specimens were crept to successive points along the creep curve. The minimum creep rate was used as an index of creep strength. The following results and conclusions were derived from this phase of the investigation:

1. The compositional dependence of the minimum creep rate at 300° C revealed a marked increase in creep strength at compositions just inside the two-phase boundary. This temperature and composition range corresponded to the area of retarded rate of age hardening noted in the kinetic contour plot.

2. Microscopical observations confirmed, in general, the same mechanisms of deformation and the same sequence of deformation markings with temperature and composition as recorded for pure aluminum. Gayler's "light phenomenon" was found to occur as greatly enlarged grain-boundary regions in which reprecipitation assumed new orientations different from those in the contiguous grains.

3. The effects of aging on the minimum creep rate of single-phase alloys were compared by means of the Larson-Miller parameter and by the Z-parameter as advocated by Dorn for creep and tensile correlations. A hypothetical curve of stress versus parameter for single-phase alloys in the two-phase field was obtained by extrapolating from the single-phase region. This curve was compared with the experimentally determined curve of stress versus parameter for two-phase alloys which were stressed and aged simultaneously. For stresses up to about 10,000 psi, the two-phase alloys were stronger than their single-phase (extrapolated) counterparts. However, at higher stresses an inversion in relative strengths occurred, and the single-phase alloys assumed a greater (calculated) strength. The Larson-Miller and Z-parameters for creep were shown to be equivalent functions.

Battelle Memorial Institute,
Columbus, Ohio, January 10, 1956.

APPENDIX A

DETERMINATION OF AN EFFECTIVE INITIAL GAGE LENGTH FOR CALCULATING STRAINS IN TENSILE TEST

An effective initial gage length for calculating strains in the tensile test was determined in the following way:

(1) The strain in the gage section ϵ_g resulting from tensile deformation was determined by initial l_i and final l_f measurements of the gage-mark spacings:

$$\epsilon_g = \frac{l_f - l_i}{l_i}$$

(2) This strain was not the same as that calculated from initial L_i and final L_f measurements of the shoulder-to-shoulder distance ϵ_s, since the cross-sectional area varied over the filleted portion:

$$\epsilon_s = \frac{L_f - L_i}{L_i} \neq \epsilon_g$$

(3) Therefore, a calculated initial shoulder-to-shoulder gage length L_i' was obtained from the known strain in the gage section and from the measured total elongation ΔL:

$$L_i' = \Delta L/\epsilon_g$$

(4) The difference between the measured and the calculated initial shoulder-to-shoulder distance was not the same for all specimens:

$$L_i - L_i' \neq \text{Constant}$$

(5) The effect of random variations in this difference was minimized by use of an average difference for all n specimens:

$$\overline{(L_i - L_i')} = \frac{1}{n}\sum_{1}^{n}(L_i - L_i')_n$$

(6) The effective gage length was obtained for all specimens by subtracting the average distance from the initial shoulder-to-shoulder distance:

$$L_{eff} = L_i - \overline{(L_i - L_i')}$$

REFERENCES

1. Wood, W. A., and Scrutton, R. F.: Mechanism of Primary Creep in Metals. The Jour. Inst. Metals, vol. 77, pt. 5, July 1950, pp. 423-434.

2. Wood, W. A., and Rachinger, W. A.: The Mechanism of Deformation in Metals, with Special Reference to Creep. The Jour. Inst. Metals, vol. 76, pt. 3, Nov. 1949, pp. 237-253.

3. Howard, Robert T., and Cohen, Morris: Quantitative Metallography by Point-Counting and Lineal Analysis. Trans. Am. Inst. Min. and Metall. Eng., vol. 172, 1947, pp. 413-426.

4. Anon.: Metals Handbook. A.S.M. (Cleveland), 1948, p. 1159.

5. Servi, Italio S., and Grant, Nicholas J.: Creep and Stress-Rupture Behavior of Aluminum as a Function of Purity. Trans. Am. Inst. Min. and Metall. Eng., vol. 191, 1951, pp. 909-916.

6. Giedt, W. H., Sherby, O. D., and Dorn, J. E.: The Effect of Dispersions on Creep Properties of Aluminum-Copper Alloys. Trans. A.S.M.E. vol. 77, no. 1, Jan. 1955, pp. 57-63.

7. Sherby, O. D., and Dorn, J. E.: Creep Correlations in Alpha Solid Solutions of Aluminum. Jour. Metals, vol. 4, no. 9, Sept. 1952, pp. 959-964.

8. Chang, H. C., and Grant, N. J.: Observations of Creep in the Grain Boundary in High-Purity Aluminum. Jour. Metals, vol. 4, no. 6, June 1952, pp. 619-625.

9. Gayler, M. L. V.: The Ageing of a High-Purity Aluminium Alloy Containing 4 Per Cent of Copper. The Jour. Inst. Metals, vol. 72, pt. 4, Apr. 1946, pp. 243-263.

10. Polmear, I. J., and Hardy, H. K.: Some Metallographic Observations on Aged Aluminium-Copper Alloys. The Jour. Inst. Metals, vol. 81, pt. 8, Apr. 1953, pp. 427-431.

11. Phillips, V. A.: Discussion on Precipitation-Hardening. The Jour. Inst. Metals, vol. 82, pt. 12, Aug. 1953, p. 612.

12. Stanford, Edwin Garnet: The Creep of Metals and Alloys. Temple Press Ltd. (London), 1949.

13. Larson, F. R., and Miller, James: A Time-Temperature Relationship for Rupture and Creep Stress. Trans. A.S.M.E., vol. 74, no. 5, July 1952, pp. 765-775.

14. Heimerl, George J.: Time-Temperature Parameters and an Application to Rupture and Creep of Aluminum Alloys. NACA TN 3195, 1954.

15. Zener, C., and Hollomon, J. H.: Plastic Flow and Rupture of Metals. Trans. A.S.M., vol. 33, 1944, pp. 163-215.

16. Sherby, O. D., Orr, R. L., and Dorn, J. E.: Creep Correlations of Metals at Elevated Temperatures. Jour. Met., vol. 6, no. 1, Jan. 1954, pp. 71-80.

17. Hardy, H. K.: The Ageing Characteristics of Binary Aluminium-Copper Alloys. The Jour. Inst. Metals, vol. 79, pt. 5, July 1951, pp. 321-369.

18. Gayler, M. L. V.: The Ageing of High-Purity 4 Per Cent Copper-Aluminium Alloy. The Jour. Inst. Metals, vol. 66, pt. 3, Mar. 1940, pp. 67-84.

19. Sully, A. H., and Hardy, H. K.: Some Metallographic Observations of the Creep of Aluminium-Copper Alloys. The Jour. Inst. Metals, vol. 82, pt. 6, Feb. 1954, pp. 264-265.

20. Wilms, G. R.: Some Observations on the Tertiary Stage of Creep of High-Purity Aluminum. Jour. Metals, vol. 6, no. 11, Nov. 1954, pp. 1291-1296.

21. Calvet, Jean, Jacquet, Pierre, and Guinier, André: The Age-Hardening of a Copper-Aluminium Alloy of Very High Purity. The Jour. Inst. Metals, vol. 65, no. 2, 1939, pp. 121-137.

22. Borelius, G., Andersson, J., and Gullberg, K.: Thermal Investigations on Constitution and Aging of Aluminum-Copper Alloys With Low Copper Content. Ing. Vetenskaps Akad. Handlingar, no. 169, 1943, pp. 1-38. Quoted by Hardy, H. K., and Heal, T. J.: Progress in Metal Physics. Vol. V. Pergamon Press, Ltd. (London), 1954, p. 236.

23. Swindells, N., and Sykes, C.: Specific Heat-Temperature Curves of Some Age-Hardening Alloys. Proc. Roy. Soc. (London), ser. A, vol. 168, no. A-933, Oct. 25, 1938, pp. 237-264.

24. Meijering, J. L.: Calculs thermodynamiques concernant la nature de zones Guinier-Preston dans les alliages aluminium-cuivre. Rev. Metallurgie, t. 49, pt. 12, Dec. 1952, pp. 906-910.

25. Silcock, J. M., Heal, T. J., and Hardy, H. K.: Structural Ageing Characteristics of Binary Aluminum-Copper Alloys. The Jour. Inst. Metals, vol. 82, pt. 6, Feb. 1954, pp. 239-248.

26. Shaw, R. B., Shepard, L. A., Starr, C. D., and Dorn, J. E.: The Effect of Dispersions on the Tensile Properties of Aluminum-Copper Alloys. Trans. A.S.M., vol. 45, 1953, pp. 255-274.

27. Guinier, A.: Formation et développement des zones et des précipités au sein des solutions solides supersaturées. (Formation and Development of Zones and of Precipitates From Supersaturated Solid Solutions.) Zs. Elektrochemie, vol. 56, no. 5, May 1952, pp. 468-473.

28. Roberts, C. S.: Interaction of Precipitation and Creep in Mg-Al Alloys. Trans. A.I.M.E., vol. 206, 1956, pp. 146-148; discussion, pp. 1410-1412.

29. Wassermann, G., and Weerts, J.: Über den Mechanismus der $CuAl_2$-Ausscheidung in einer aushärtbaren Kupfer-Aluminium-Legierung. (On the Mechanism of Precipitation of $CuAl_2$ in an Age-Hardenable Aluminum-Copper Alloy.) Metallwirtschaft, vol. 14, no. 31, Aug. 1935, pp. 605-609.

30. Preston, G. D.: The Diffraction of X-Rays by an Age-Hardening Alloy of Aluminium and Copper. The Structure of an Intermediate Phase. Phil. Mag., Suppl., vol. 26, ser. 7, no. 128, Nov. 1938, pp. 855-871.

31. Dehlinger, U.: Chemische Physik der Metalle und Legierungen. (Chemical Physics of Metals and Alloys.) Akademische Verlags (Leipzig), 1939.

32. Scheil, E.: Remarks on the Concentration of Nuclei Upon Precipitation from Supersaturated Solid Solutions. Zs. Metallkunde, Bd. 43, Heft 1, Jan. 1942, pp. 40-42.

33. Scheil, E.: Über die Irreversibilität der Eisen-Nickel-Legierungen. Archiv. Eisenhüttenwesen, Bd. 24, Heft 3-4, Mar.-Apr. 1953, pp. 153-160.

34. Masing, G., and Nickel, O.: Keimbildung bei Umwandlungen in den irreversiblen Eisen-Nickel-Legierungen. Archiv. Eisenhüttenwesen, Bd. 24, Heft 3-4, Mar.-Apr. 1953, pp. 143-151.

35. Gerlach, W.: Die heterogene Ausscheidung im System Gold-Nickel. Zs. Metallkunde, Bd. 40, Heft 8, Aug. 1949, pp. 281-289.

36. Underwood, E. E.: Precipitation in Gold-Nickel Alloys. Sc.D. Thesis, M.I.T., 1954.

37. Saulnier, M. A.: Discussion on Precipitation-Hardening. The Jour. Inst. Metals, vol. 82, pt. 12, Aug. 1953, p. 611.

38. Kempf, L. W., and Hopkins, H. L.: Density Changes in Solid Aluminum Alloys. Trans. Am. Inst. Min. and Metall. Eng., vol. 122, 1936, pp. 266-281; discussion by Brick, R. M., and Smith, A. J., pp. 281-283.

39. Sherby, Oleg D., and Dorn, John E.: Some Observations on Correlations Between the Creep Behavior and the Resulting Structures in Alpha Solid Solutions. Jour. Metals, vol. 5, no. 2, sec. 2 (Trans. Supp.), Feb. 1953, pp. 324-330.

40. Sherby, Oleg D., Goldberg, Alfred, and Dorn, John E.: Effect of Prestrain Histories on the Creep and Tensile Properties of Aluminum. Trans. A.S.M., vol. 46, 1954, pp. 681-700.

TABLE 1.- SPECTROGRAPHIC AND CHEMICAL ANALYSES

OF ALUMINUM-COPPER ALLOYS

Nominal composition, weight percent copper	Chemical analysis, weight percent copper	Spectrographic analysis, parts per million			
		Si (a)	Fe	Pb	Mg
1	0.99	20	20	[b] <10	1.0
2	1.95	20	[b] <20	(b)	1.0
3	2.96	20	[b] <20	(b)	1.0
4	3.97	20	[b] <20	20	1.0

[a] Silicon pickup possible from electrode.

[b] Not detected.

TABLE 2.- TABULATION OF CREEP DATA

IN ALUMINUM-COPPER ALLOYS

Composition, weight percent copper	Testing temperature, °C	Initial creep stress, psi	Number of specimens used	Location on equilibrium diagram
1	300	2,400	1	Two-phase
	300	2,000	1	Do.
	300	1,700	1	Do.
	419	200	1	Single-phase
	430	200	2	Do.
	457	200	1	Do.
2	200	7,500	4	Two-phase
	200	7,000	1	Do.
	200	6,000	2	Do.
	300	2,400	5	Two-phase
	300	2,050	3	Do.
	300	1,700	3	Do.
	400	1,700	5	Two-phase
	400	1,235	4	Do.
	400	790	4	Do.
	430	1,000	1	Single-phase
	460	353	1	Single-phase
	460	251	1	Do.
	460	201	1	Do.
	500	362	1	Single-phase
	500	202	1	Do.
	500	140	1	Do.
	540	206	1	Single-phase
	540	140	1	Do.
	540	86	1	Do.
3	300	3,200	4	Two-phase
	300	2,800	1	Do.
	300	2,400	3	Do.
4	300	4,000	1	Two-phase
	300	3,200	1	Do.
	300	2,800	1	Do.

TABLE 3.- TABULATION OF AGE-HARDENING DATA

IN ALUMINUM-COPPER ALLOYS

[Hardness data were obtained from a Vicker's hardness tester with a 10-kilogram load]

Composition, weight percent copper	Average initial hardness (a)	Maximum hardness at reaction temperatures, °C, of -				Time, min, to maximum hardness at reaction temperatures, °C, of -			
		200	220	300	400	200	220	300	400
1	27.5	----	-----	29	----	-----	-----	25	----
2	44.4	50.8	~50.3	~50	50.7	4,100	1,250	37	52
3	66.4	68	-----	63	63.5	1,100	-----	16	3.7
4	81.7	81.7	-----	76.6	74	1,300	-----	17	1.4

[a]Alloys were quenched from 540° C into water at room temperature.

TABLE 4.- TABULATION OF DATA PERTAINING TO CREPT SPECIMENS OF ALUMINUM ALLOYS

Specimen	Test temperature, °C	Initial creep stress, psi	ASTM grain size	Time of creep run, min.	Total creep strain, percent	Final condition	Ultimate tensile strength, psi	Hardness readings, DPHN		Remarks
								Gage section	Shoulders	
Alloys containing 1 percent copper										
1-2-5	457	200	-2	2,860	18.4	Water-quenched	----------	----	----	Single-phase creep
1-2-6	429	200	1 + 0	4,360	19.4	-----do.------	----------	----	----	Do.
1-2-7	430	200	0	3,122	14.1	-----do.------	----------	----	----	Do.
1-2-4	419	200	1	11,205	12.1	-----do.------	----------	----	----	Do.
1-2-1	302	2,400	1	72	20.8	-----do.------	13,190 ± 390	24.1	24.7	----------
1-2-2	303	2,000	1	148	16.8	-----do.------	12,120 ± 400	26.5	24.1	----------
1-2-3	301	1,700	1	483	22.9	-----do.------	13,200 ± 700	26.8	25.1	----------
1-2-8	26	-----	-1	------	----	-----do.------	14,410	----	----	Tensile test only
Alloys containing 2 percent copper										
2-2-25	540	206	1 + 0	381	20.6	----------	----------	-----	----	Single-phase creep
2-2-26	540	140	2 + 1	1,306	23.0	Water-quenched	----------	----	----	Do.
2-2-24	540	85.6	1	9,570	23.3	-----do.------	----------	----	----	Do.
2-2-18	500	362	-1 + 0	215	23.7	-----do.------	----------	----	----	Do.
2-2-19	500	201.5	-1 + 0	1,733	24.0	-----do.------	----------	----	----	Do.
2-2-20	500	139.5	1 + 0	9,750	31.8	-----do.------	----------	----	----	Do.
2-2-21	460	353	1 + 0	1,341	30.2	----------	----------	----	----	Do.
2-2-22	460	251	1	2,875	21.4	----------	----------	----	----	Do.
2-2-23	460	201	1	7,465	25.6	----------	----------	----	----	Do.
2-3-48	430	1,000	1 + 2	40	13.4	-----do.------	----------	----	----	Do.
2-2-4	400	1,766	1	39	1.3	-----do.------	19,190	41.6	50.9	----------
2-2-2	400	1,725	1	75	7.6	-----do.------	19,735	40.4	42.0	----------
2-2-6	400	1,693	1	149	33.0	Ruptured	----------	35.9	35.2	----------
2-2-3	400	1,689	1	50	2.9	Water-quenched	19,790	40.4	43.4	----------
2-2-5	400	1,685	1	22	.8	-----do.------	19,700	45.4	41.5	----------
2-2-10	403	1,316	1	199	20.0	-----do.------	17,550	35.3	36.8	----------
2-2-12	400	1,260	1	43	1.6	-----do.------	23,050	48.0	43.9	----------
2-2-8	402	1,243	1	202	5.9	-----do.------	----------	51.8	39.2	----------
2-2-7	400	1,236	1	236	46.0	-----do.------	----------	35.8	34.9	----------
2-2-11	403	1,215 ± 53	1	94	1.9	-----do.------	20,360	39.8	38.6	----------
2-2-9	403	1,197 ± 10	1	139	12.5	-----do.------	18,400	36.8	36.5	----------
2-2-15	400	927	1	65	1.4	-----do.------	21,450	43.9	45.5	----------
2-2-14	400	798	1	281	2.9	-----do.------	16,910	34.6	34.7	----------
2-2-16	400	793	1	180	1.7	-----do.------	20,000	37.6	36.8	----------
2-2-13	403	787	1	620	7.7	-----do.------	19,320	38.9	35.7	----------
2-2-17	400	782	1	70	1.0	-----do.------	22,000	40.0	38.7	----------
2-2-30	300	2,400	1	3,261	13.3	Ruptured	----------	37.6	38.5	----------
2-2-33	300	2,399	1	3,803	10.0	-----do.------	----------	38.0	38.7	----------
2-2-32	300	2,404	1	2,913	1.9	Water-quenched	21,000	41.0	41.7	----------
2-2-31	300	2,400 ± 100	1 + 0	508	2.0	-----do.------	----------	41.6	43.2	----------
2-2-34	300	2,300 ± 150	1 + 0	586	1.1	-----do.------	21,250 ± 1,450	42.7	42.2	----------
2-3-39	300	2,400	------	115	23.0	-----do.------	----------	31.2	29.6	Overaged specimen
2-2-35	300	2,050	2 + 1	7,600	8.1	Ruptured	----------	34.1	36.7	----------
2-3-36	300	2,049	2 + 1	7,050	5.9	Water-quenched	16,150	36.4	39.4	----------
2-2-37	300	2,050 ± 30	2 + 1	2,935	1.1	-----do.------	----------	41.5	42.4	----------
2-2-27	300	1,703	1 + 0	10,697	13.5	Ruptured	----------	33.4	35.4	----------
2-2-28	300	1,698	1 + 0	8,845	1.5	Water-quenched	18,250	34.7	34.0	----------
2-2-29	300	1,700	2 + 1	3,995	1.0	-----do.------	19,780	37.6	37.0	----------
2-3-42	200	7,500	2 + 1	3,428	11.1	-----do.------	----------	52.8	49.3	----------
2-3-43	199	7,500	2 + 1	4,395	8.2	Ruptured	----------	55.4	43.3	----------
2-3-44	199	7,500	2 + 1	1,600	4.0	Water-quenched	24,400	62.3	36.7	----------
2-3-45	199	7,502	2 + 1	420	3.8	-----do.------	----------	51.4	35.7	----------
2-3-46	200	7,000	2 + 1	8,455	6.6	-----do.------	----------	50.4	52.1	----------
2-2-40	200	6,000	2	13,805	4.1	-----do.------	19,450	49.5	51.9	----------
2-3-41	200	6,000	2 + 1	6,268	2.1	-----do.------	24,440	55.2	54.4	----------
2-3-47	26	-----	1	------	----	-----do.------	29,700	----	----	Tensile test only
Alloys containing 3 percent copper										
3-2-5	301	3,200	1 + 0	1,905	3.6	Water-quenched	----------	49.3	52.8	----------
3-2-6	300	3,200	1 + 0	1,665	2.3	-----do.------	25,200	49.1	52.2	----------
3-2-4	300	3,200	2 + 1	2,570	2.3	Ruptured	----------	48.2	50.5	----------
3-2-7	302	3,200	1	415	1.0	Water-quenched	29,160 ± 60	54.9	56.0	----------
3-2-8	302	2,800	1 + 0	4,050	5.2	-----do.------	22,105 ± 305	44.1	46.4	----------
3-2-1	300	2,400	1 + 0	11,505	2.4	Ruptured	----------	43.6	47.0	----------
3-2-2	303	2,400	1	11,147	1.8	Water-quenched	----------	44.1	47.3	----------
3-2-3	301	2,400	1	1,660	.9	-----do.------	27,220	51.4	52.8	----------
3-2-9	26	-----	0	------	----	-----do.------	36,100	----	----	Tensile test only
Alloys containing 4 percent copper										
4-2-1	302	4,000	2	1,315	6.1	Ruptured	----------	49.0	55.0	----------
4-2-2	302	3,200	2	2,747	5.1	Water-quenched	22,050 ± 750	48.4	53.8	----------
4-2-3	299	2,800	2 + 1	>7,317	>2.8	Ruptured	----------	46.6	51.7	----------
4-2-4	26	-----	1	------	----	Water-quenched	40,600	----	----	Tensile test only

TABLE 5.- X-RAY DIFFRACTION EXAMINATION OF 2-PERCENT-COPPER ALLOYS AGED AND/OR STRESSED AT 1,700 PSI AT 400° C

Specimen	Creep strain at 400° C	Time at 400° C, min	Type of X-ray pattern	Size of spots, mm	Length of areas, mm	Grains per mm (a)
2-U	0	1,470	Spot	1.2	---------	----
2-2-5	.80	22	Spot	2	---------	3.04
2-2-4	1.29	39	Spot	3	---------	3.02
2-2-3	2.89	50	Spot	6	---------	2.66
2-2-2	7.58	75	Debye arc	---	15	2.73
2-2-6	33.0	149	Debye arc	---	Very long	2.28

[a]Grain sizes were measured after creep runs. Average initial grain size was 5 grains/mm.

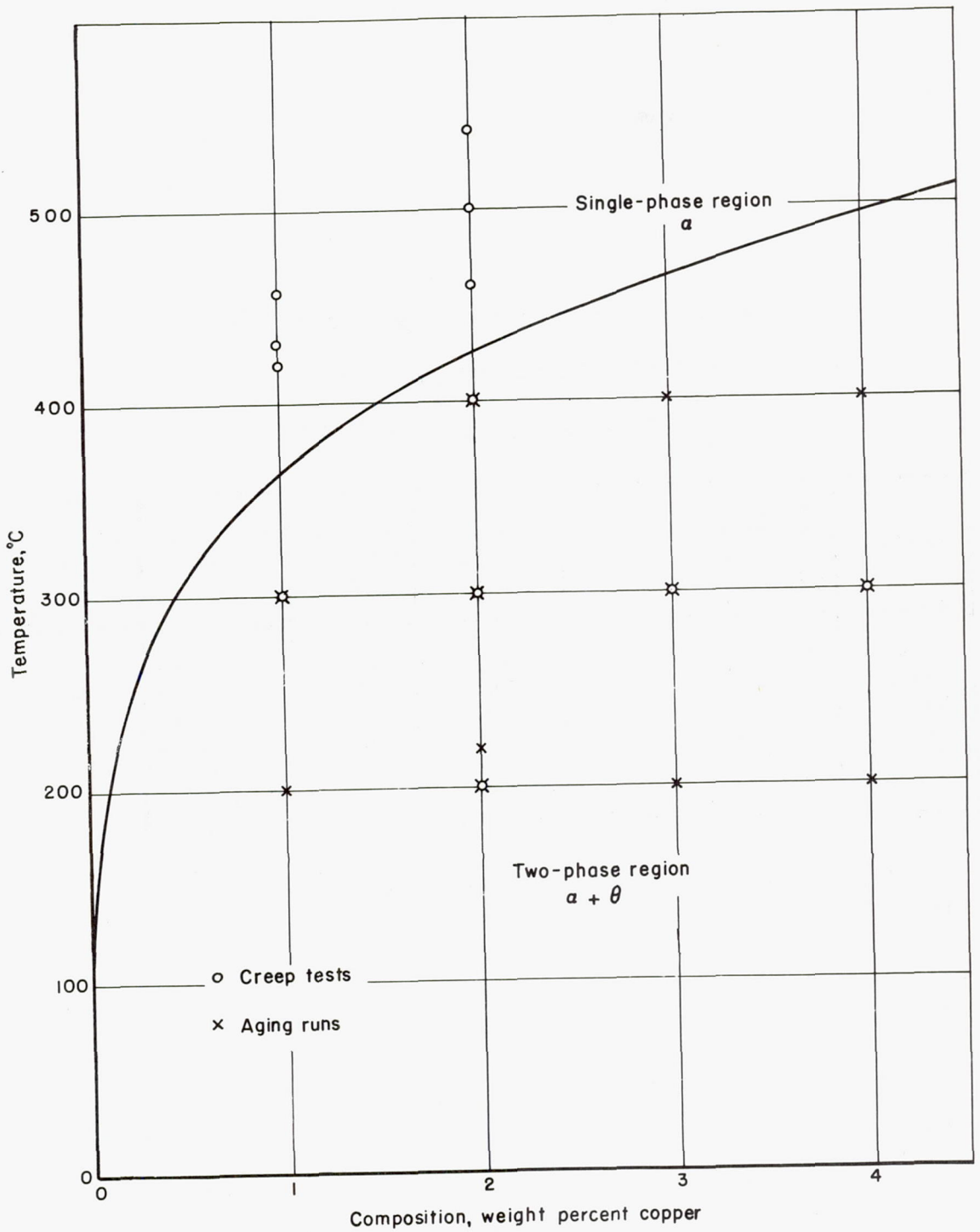

Figure 1.- Portion of equilibrium diagram for aluminum-copper alloys showing locations of creep and aging tests.

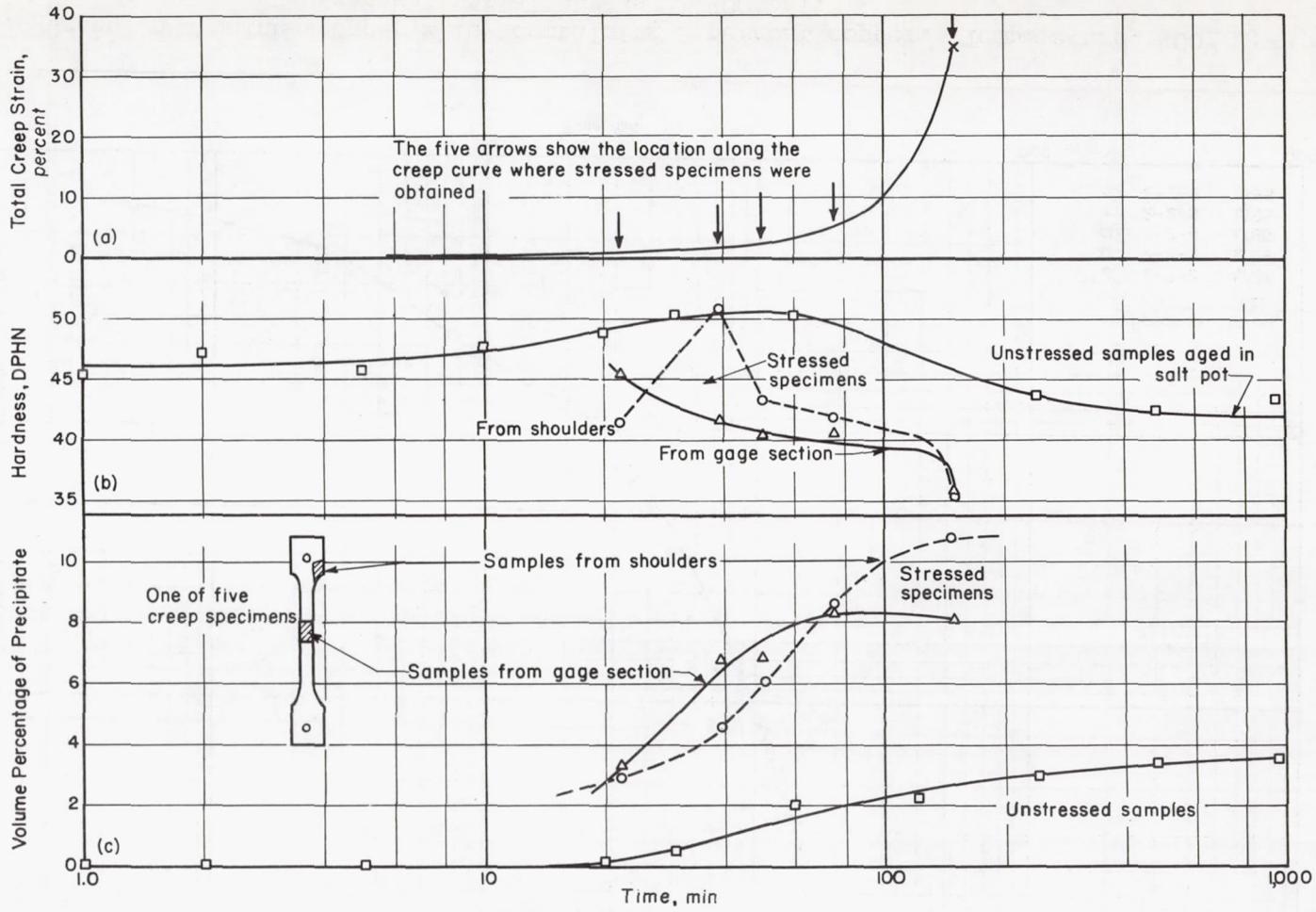

(a) Creep. Stress = 1,700 psi. (b) Age hardening. (c) Precipitation. Data obtained by point counting.

Figure 2.- Overall view of experimental method for obtaining creep, age-hardening, and precipitation data from aluminum alloys containing 2 percent copper crept and/or aged at 400° C.

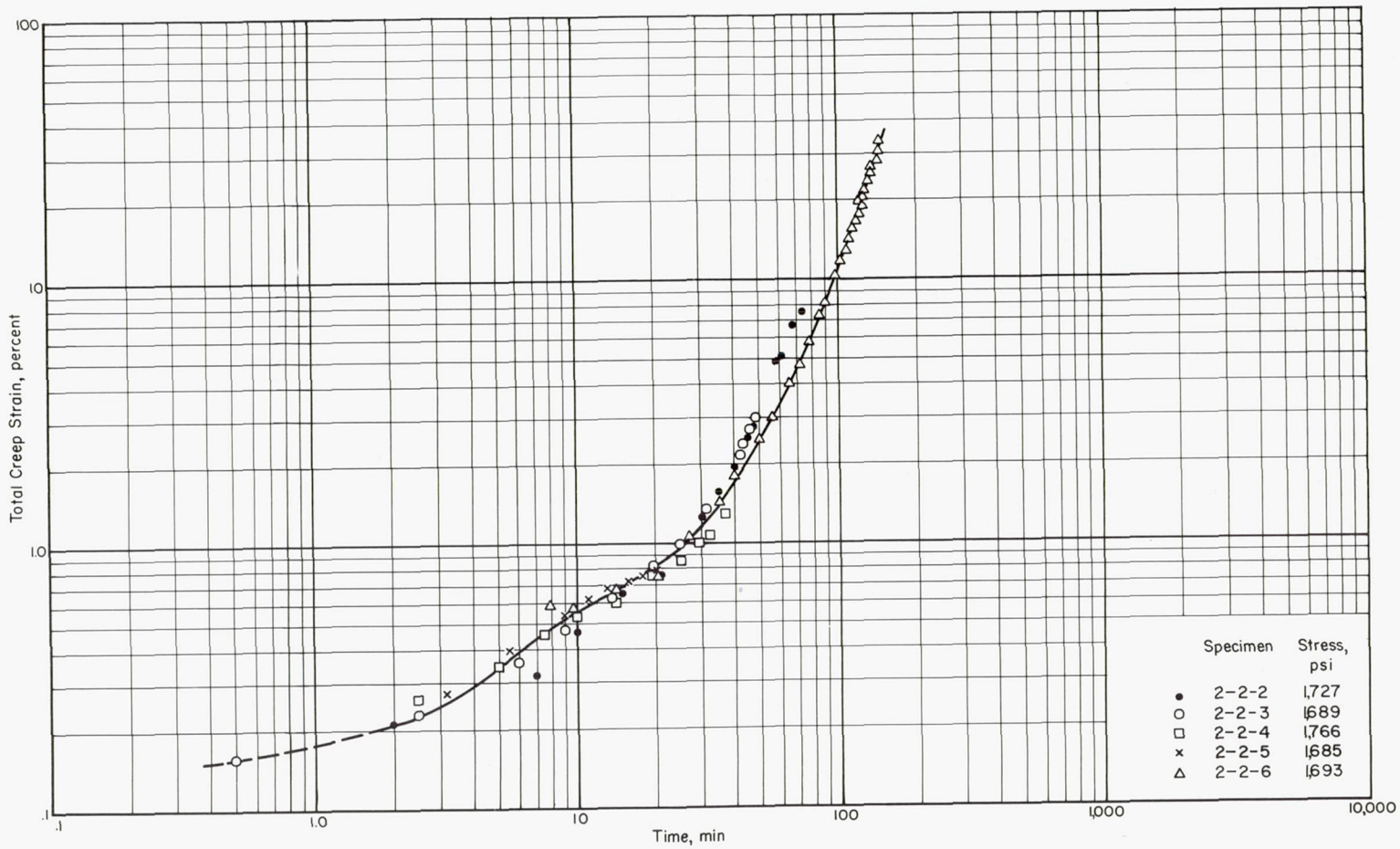

Figure 3.- Creep in aluminum-copper alloy containing 2 percent copper. Temperature, 400° C; average initial stress, 1,700 psi.

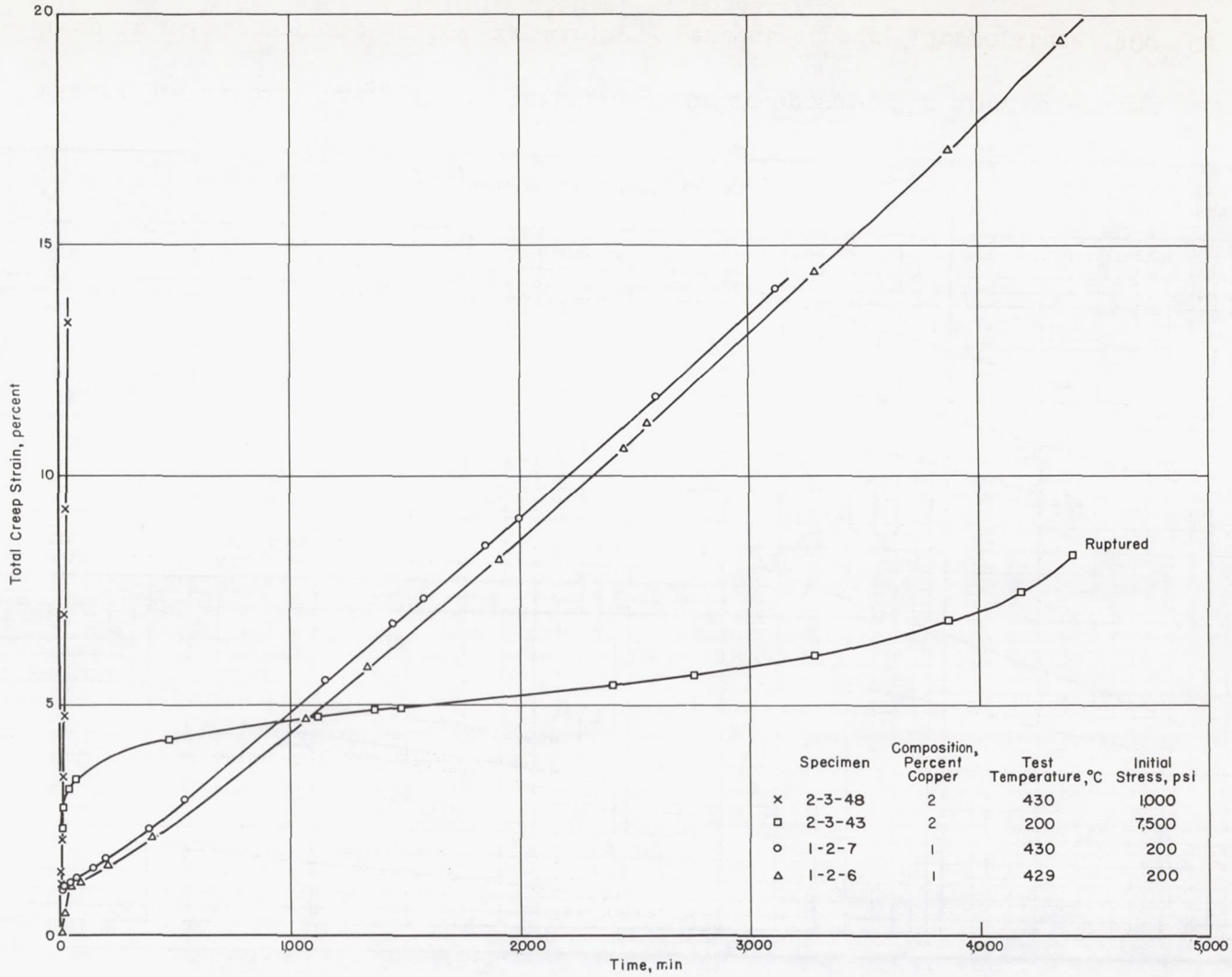

Figure 4.- Representative creep curves of some aluminum-copper alloys tested under widely varying conditions.

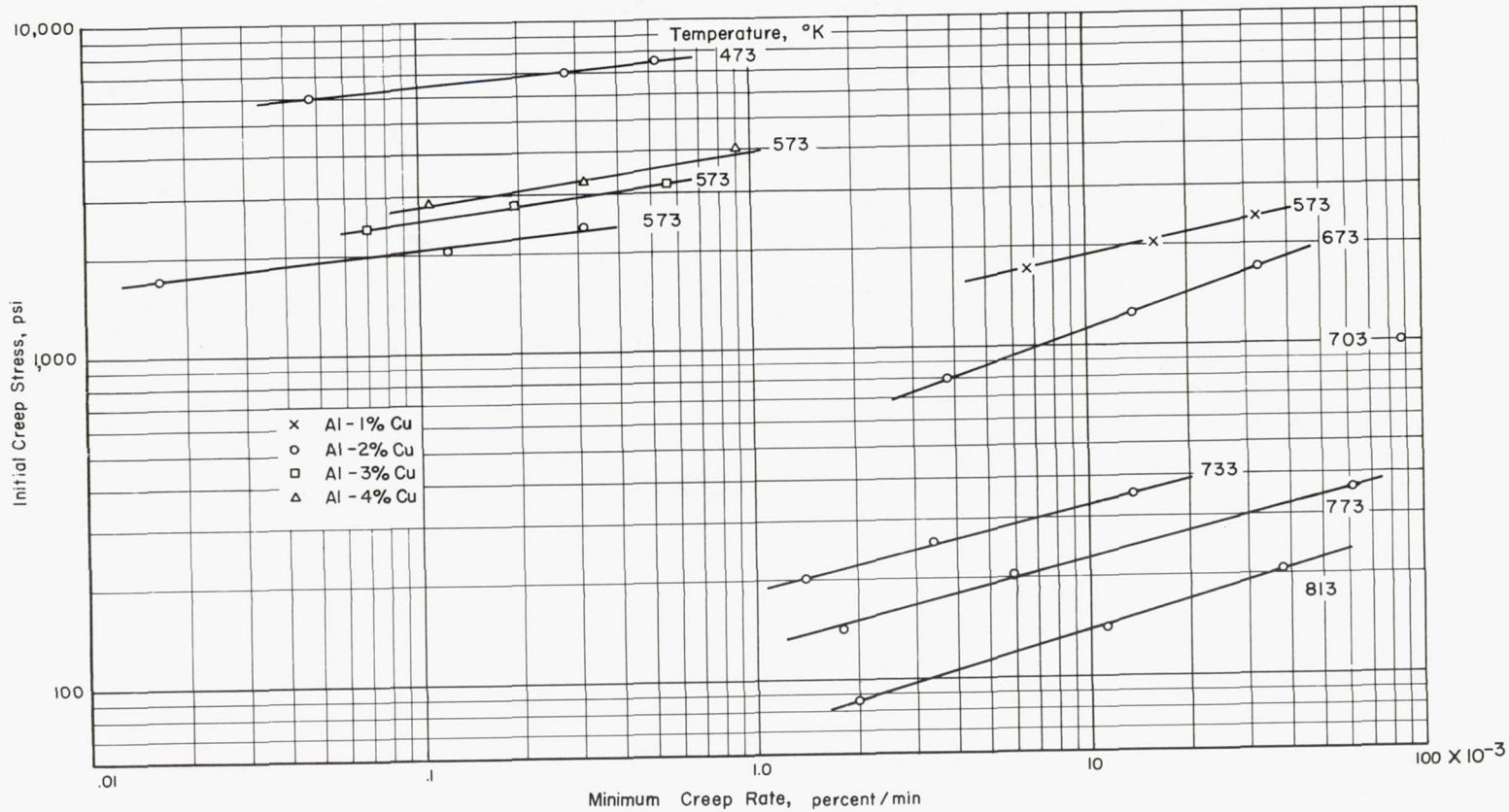

Figure 5.- Initial creep stress versus minimum creep rate for aluminum-copper alloys.

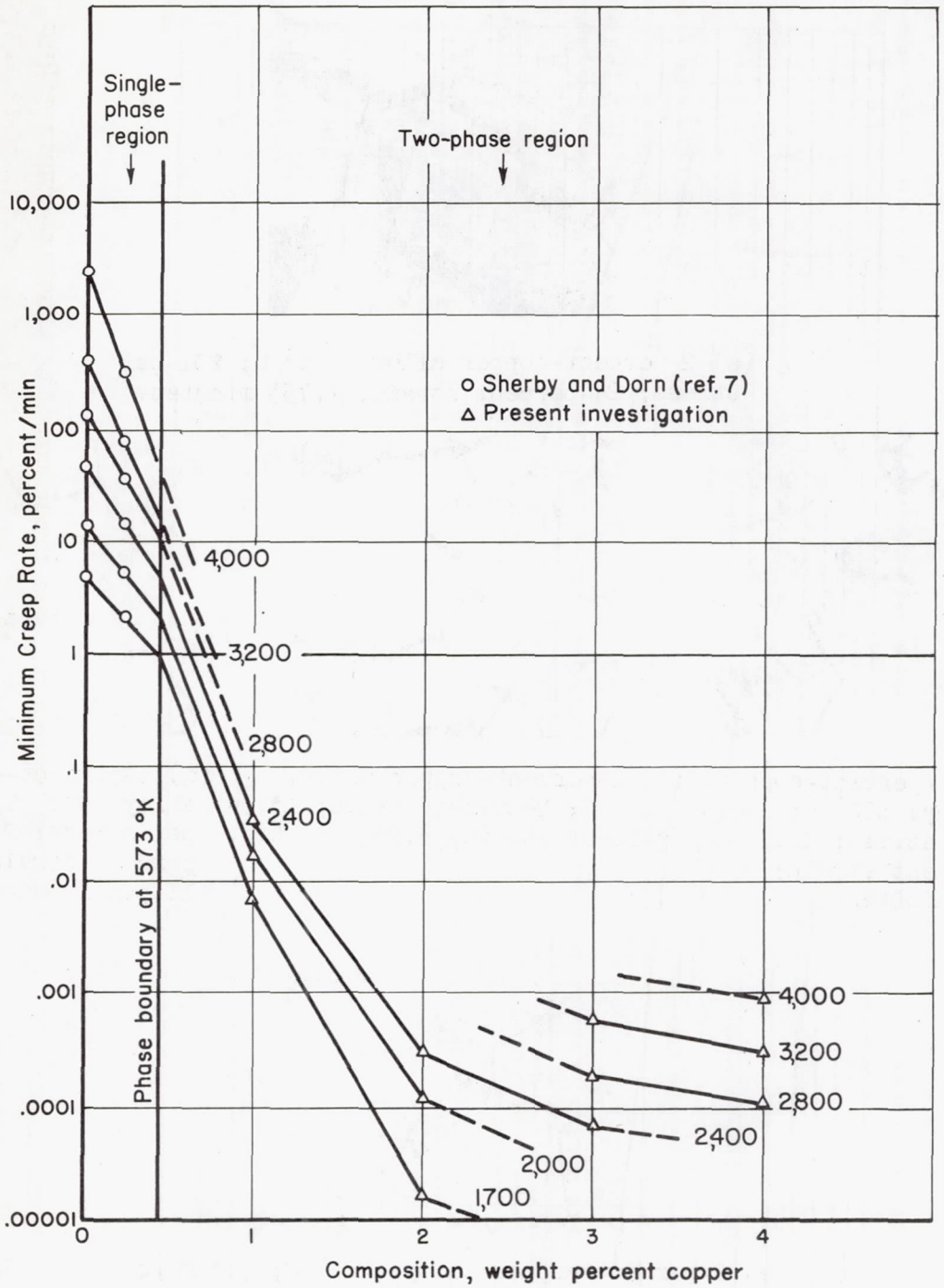

Figure 6.- Effect of stress on minimum creep rate of aluminum-copper alloys at a temperature of 573° K. Numbers represent creep stress in psi.

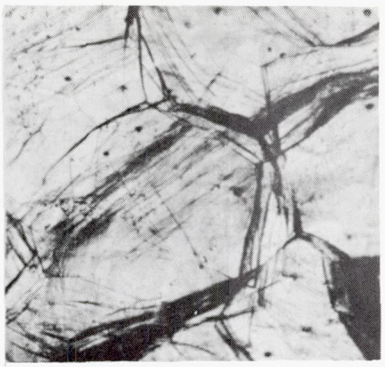

(a) 2-percent-copper alloy; 500° C; 201-psi stress; 24-percent strain; 1,733 minutes.

(b) 1-percent-copper alloy; 300° C; 2400-psi stress; 20.8-percent strain; 72 minutes.

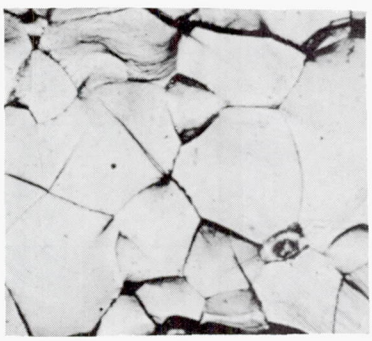

(c) 2-percent-copper alloy; 300° C; 2400-psi stress; 13.3-percent strain; 3,261 minutes.

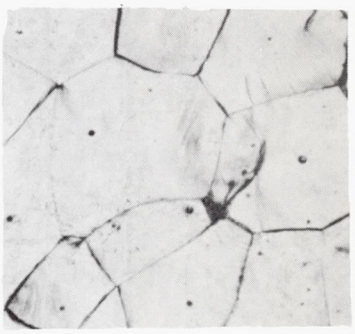

(d) 3-percent-copper alloy; 300° C; 2,400-psi stress; 2.4-percent strain; 11,585 minutes.

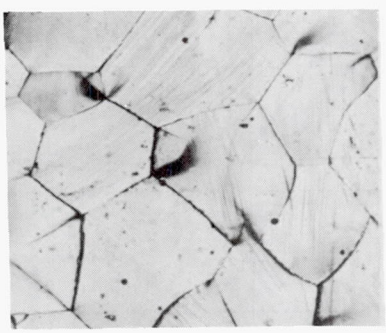

(e) 2-percent-copper alloy; 200° C; 7,500-psi stress; 11.1-percent strain; 3,428 minutes.

L-57-2575

Figure 7.- Temperature and compositional variation of surface deformation markings on crept aluminum-copper alloys. Original grain size was ASTM 1. Magnification, X50; Keller's etch.

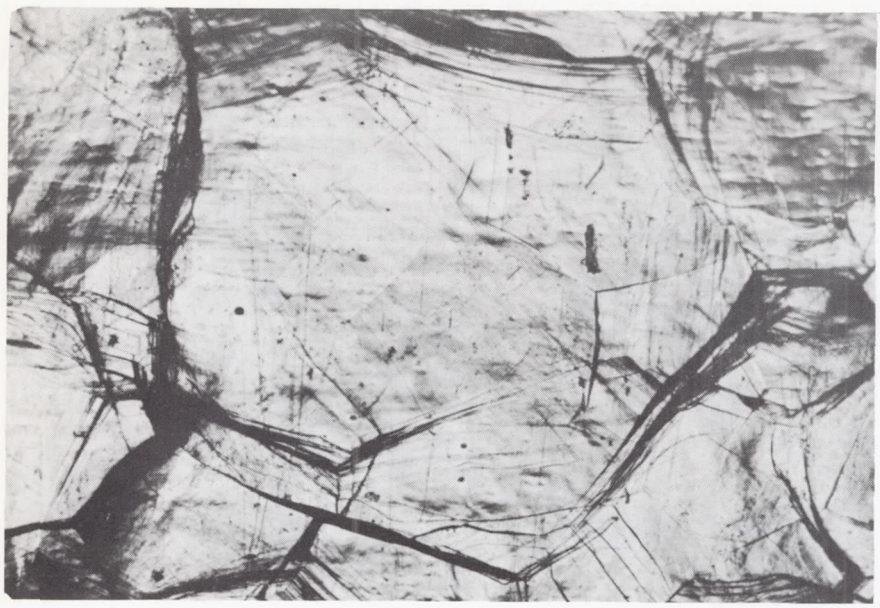

(a) Untouched surface after creep testing. Original grain size is 2.8 grains per millimeter.

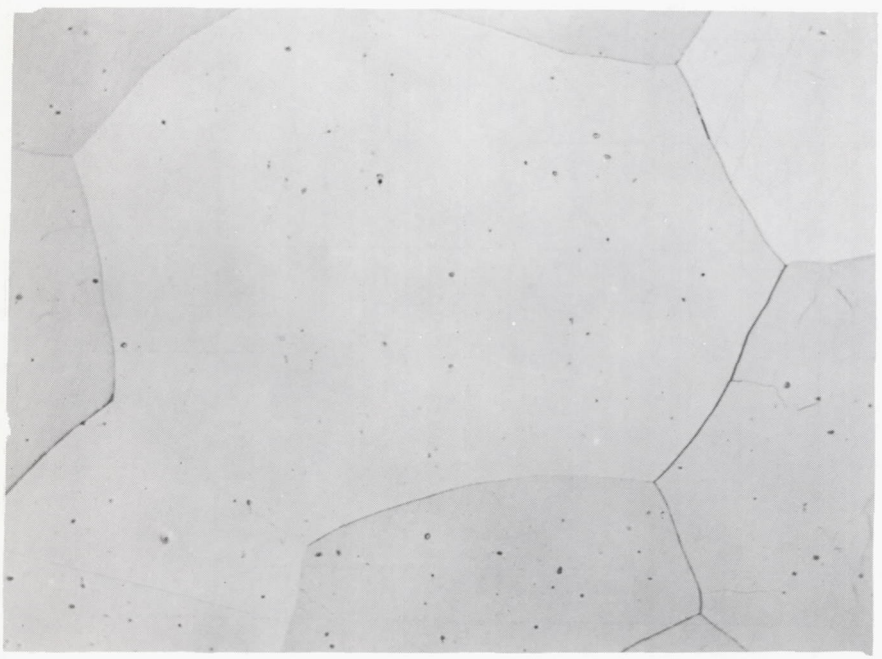

(b) Polished and etched surface; same area as above. L-57-2576
New grain size is 1.06 grains per millimeter.

Figure 8.- As-crept and polished surface of 2-percent-copper alloy stressed with 201 psi at 500° C. Magnification, X50; Keller's etch

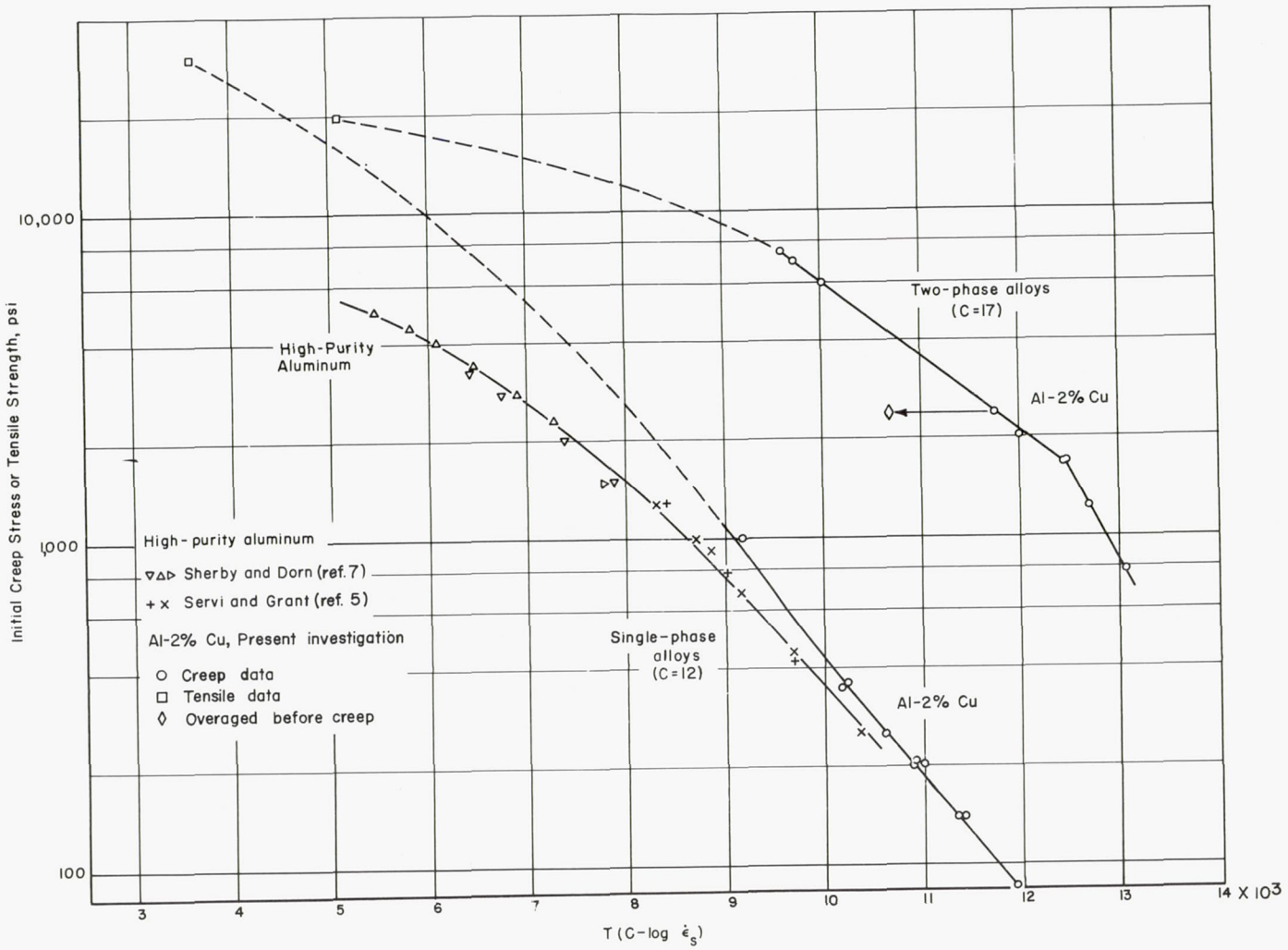

Figure 9.- Correlation of creep data by means of parameter of temperature and minimum creep rate in high-purity aluminum alloys containing 2-percent copper. T is in ^{o}K; $\dot{\epsilon}_s$, percent per minute; C, constant from equation (1).

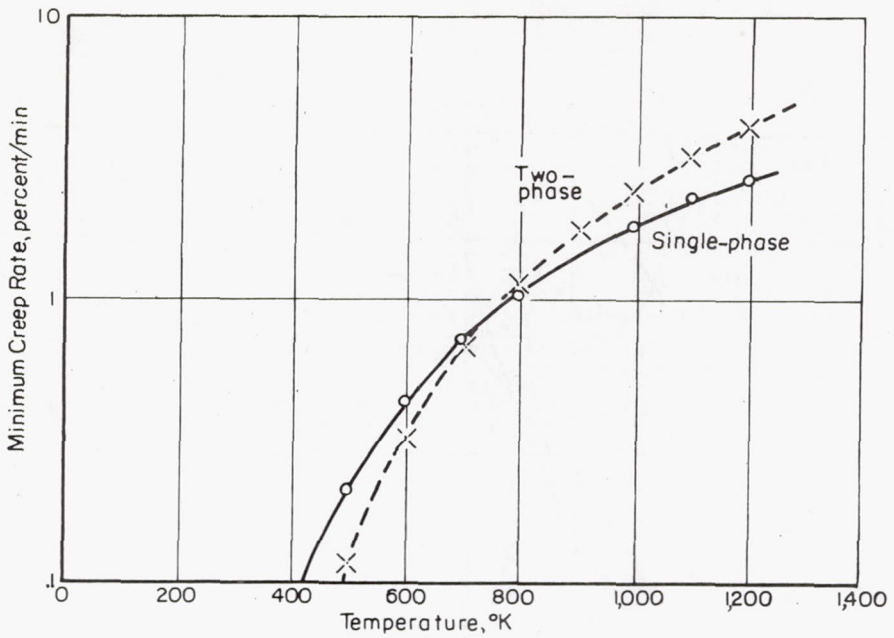

(a) Stress constant at 800 psi.

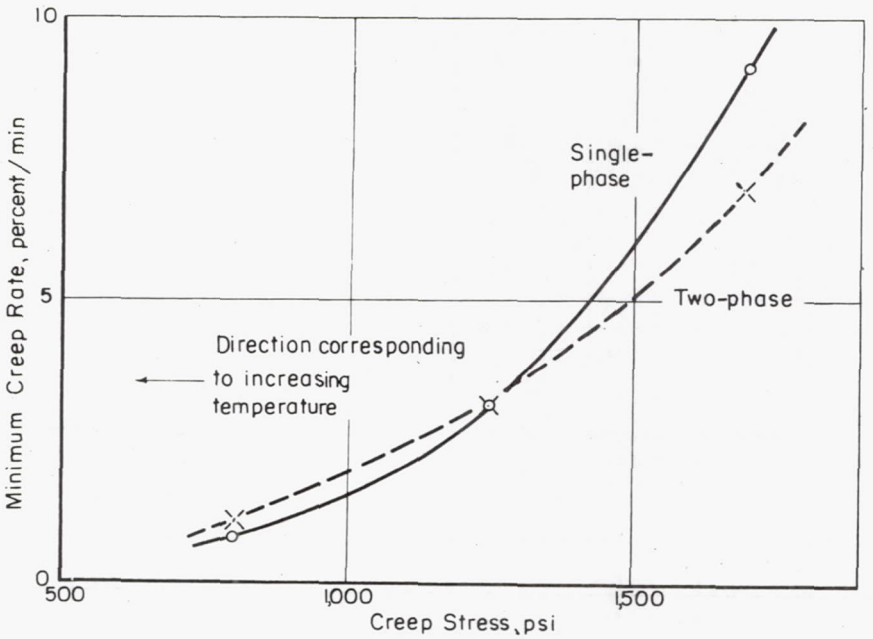

(b) Temperature constant at 770° K.

Figure 10.- Calculated minimum creep rates for single- and two-phase alloys of aluminum containing 2 percent copper.

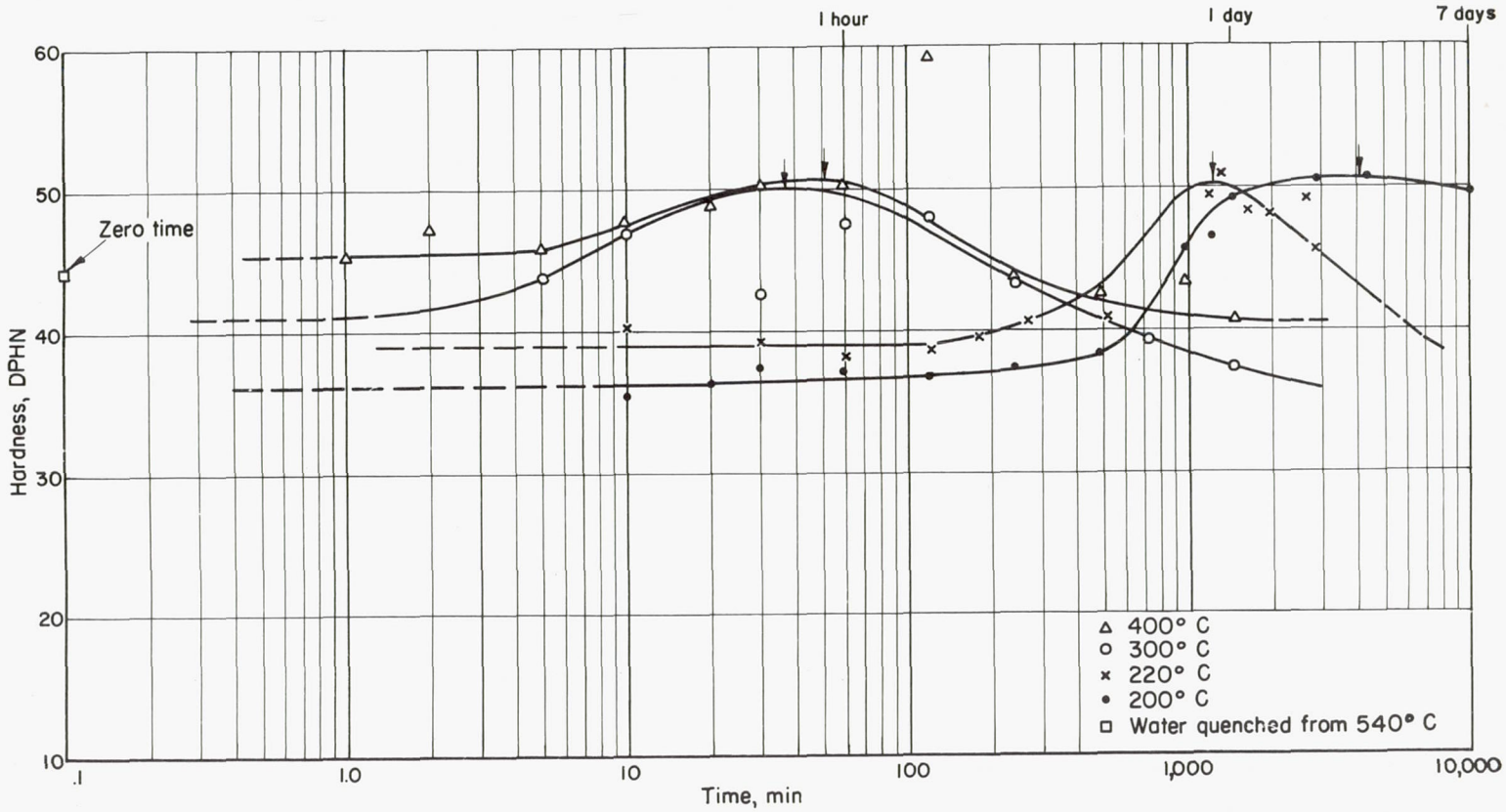

Figure 11.- Age hardening in unstressed aluminum-copper alloy containing 2 percent copper.

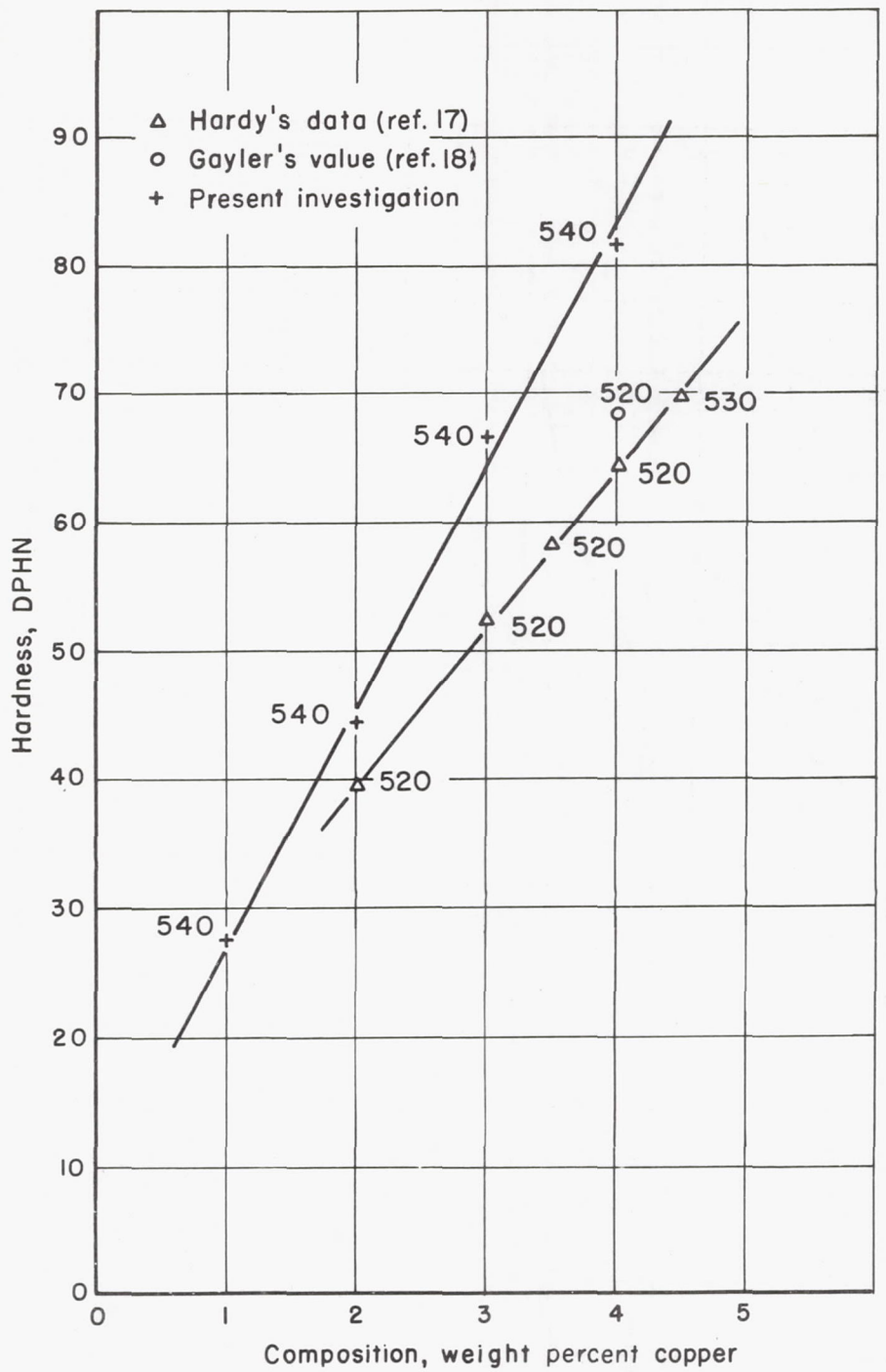

Figure 12.- Hardness of quenched aluminum-copper alloys. Numbers at data points refer to temperature, ^{o}C, from which specimens were quenched into water at room temperature.

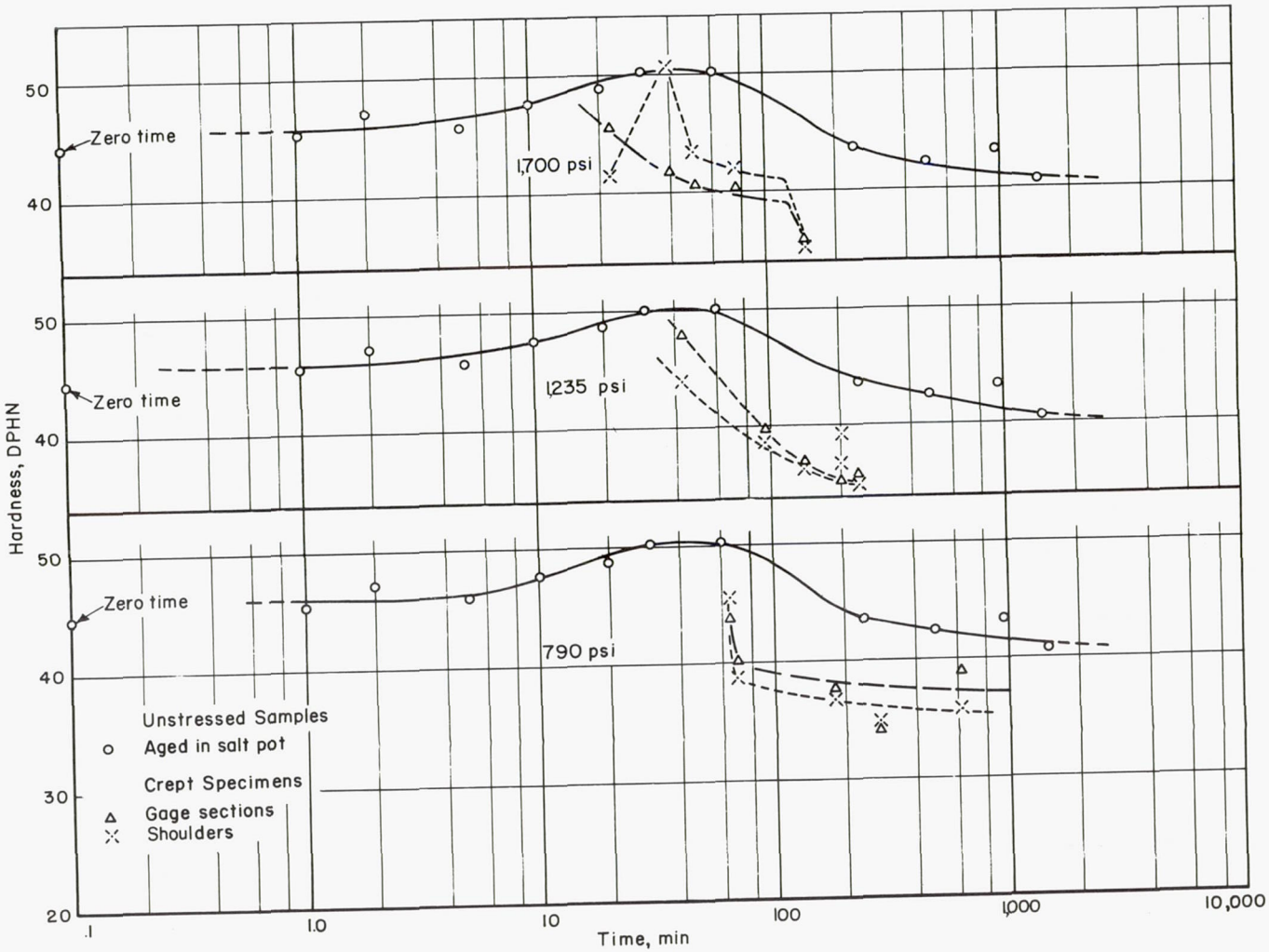

(a) Alloys aged at 400° C.

Figure 13.- Hardness versus time in stressed and unstressed aluminum alloys containing 2 percent copper.

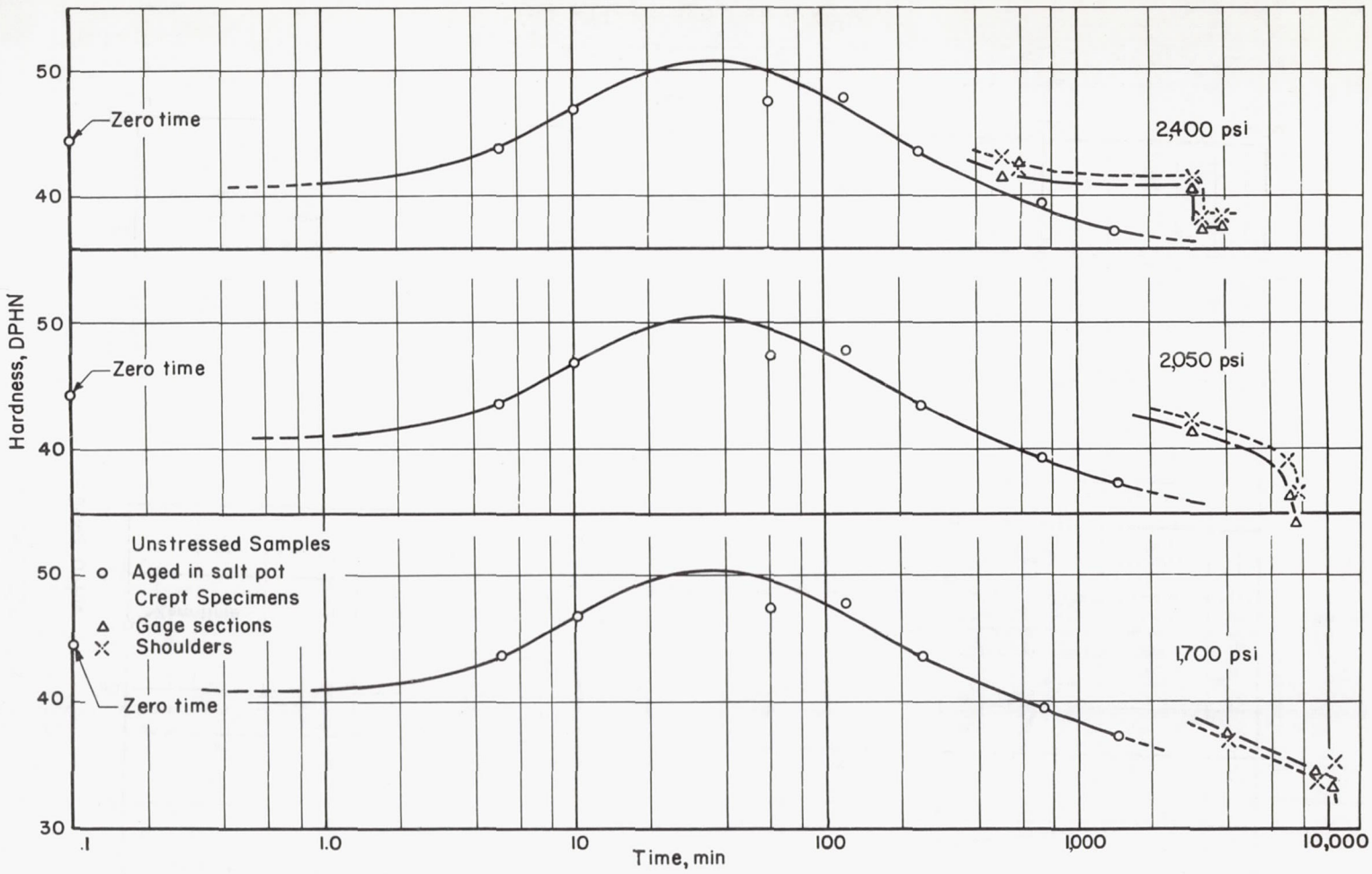

(b) Alloys aged at 300° C.

Figure 13.- Concluded.

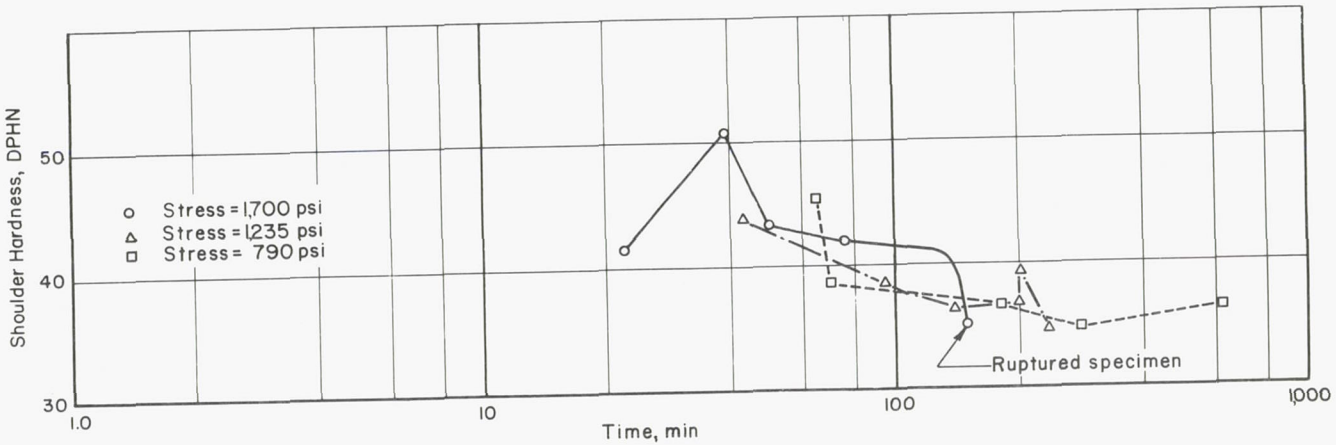

(a) Time against hardness.

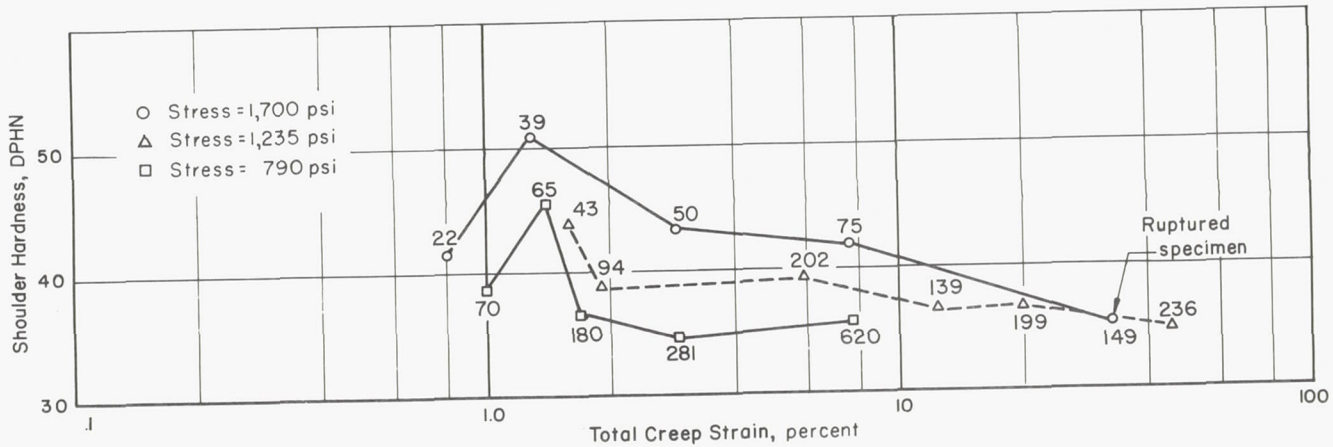

(b) Total creep strain against hardness. Numbers at data points give duration of creep test in minutes.

Figure 14.- Total creep strain and time against hardness at specimen shoulders of aluminum alloys containing 2 percent copper aged during creep at 400° C.

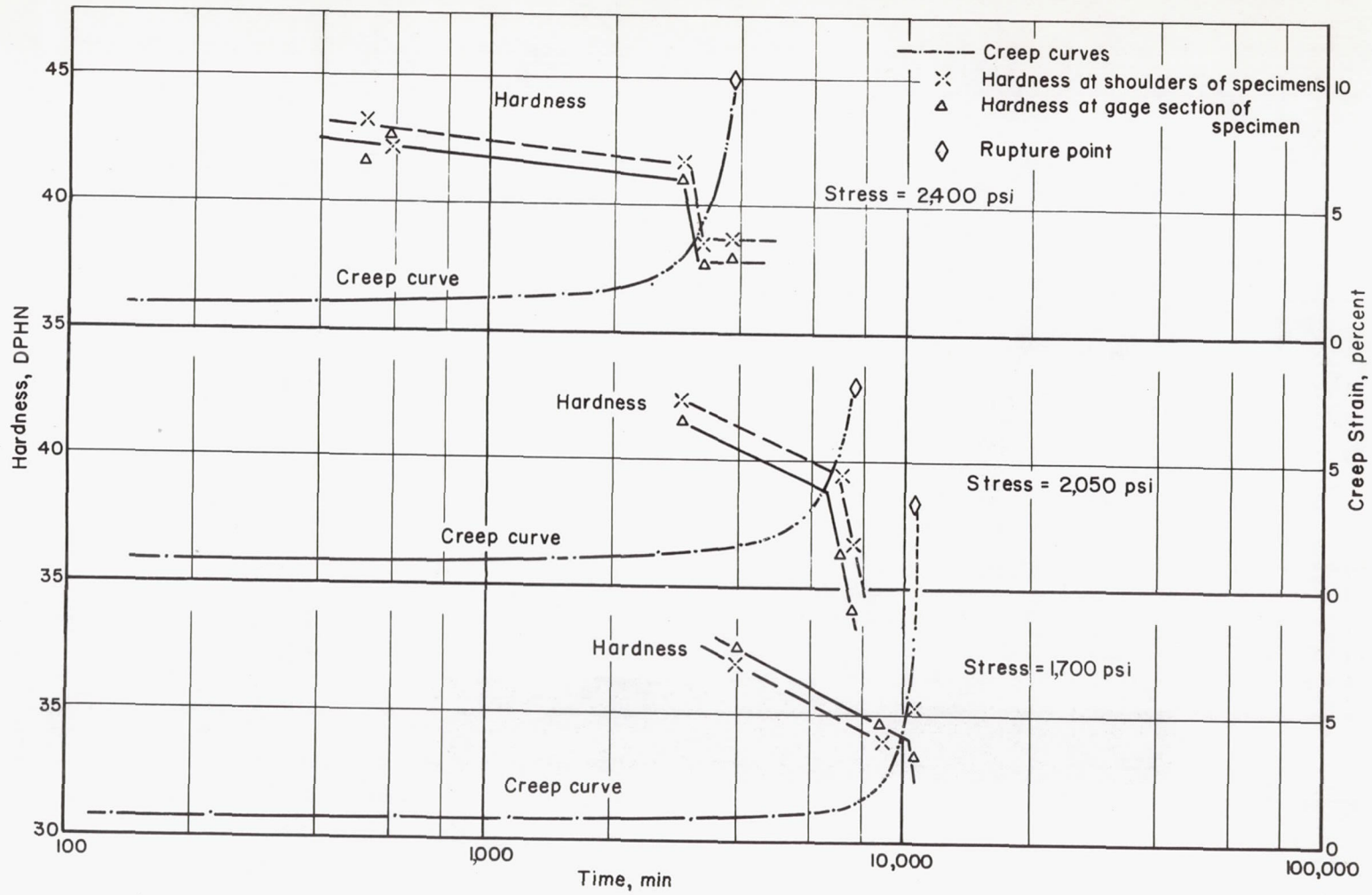

Figure 15.- Comparison of hardness and creep curves of aluminum alloys containing 2 percent copper aged and crept at 300° C.

L-57-2577

Figure 16.- Microstructure of a ruptured 2-percent-copper alloy crept under a stress of 7,500 psi at 200° C. Axis of applied stress is vertical. Magnification, X250; Keller's etch.

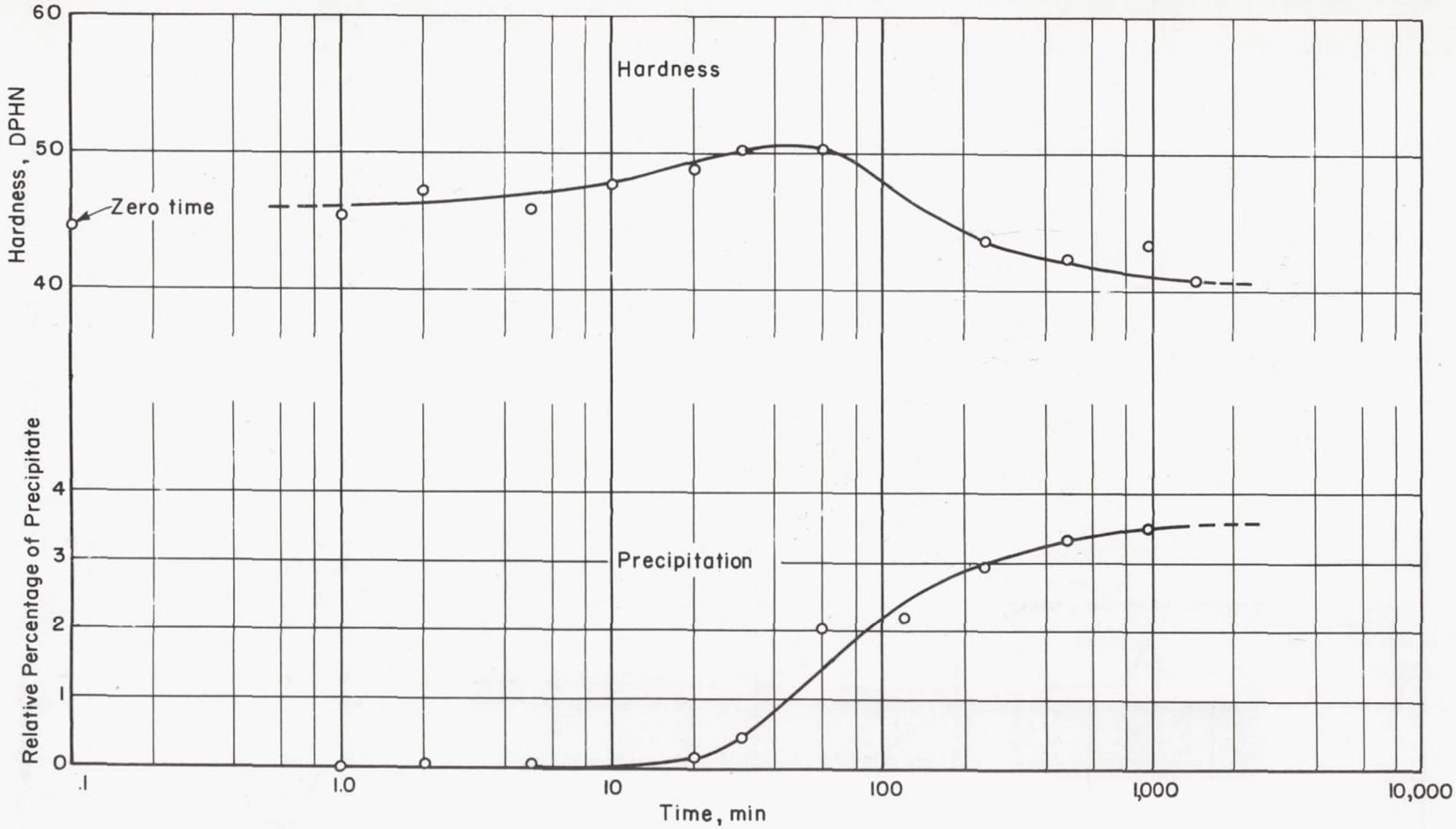

(a) Unstressed alloys aged at 400° C.

Figure 17.- Comparison of hardness and amount of precipitate aluminum alloys containing 2 percent copper.

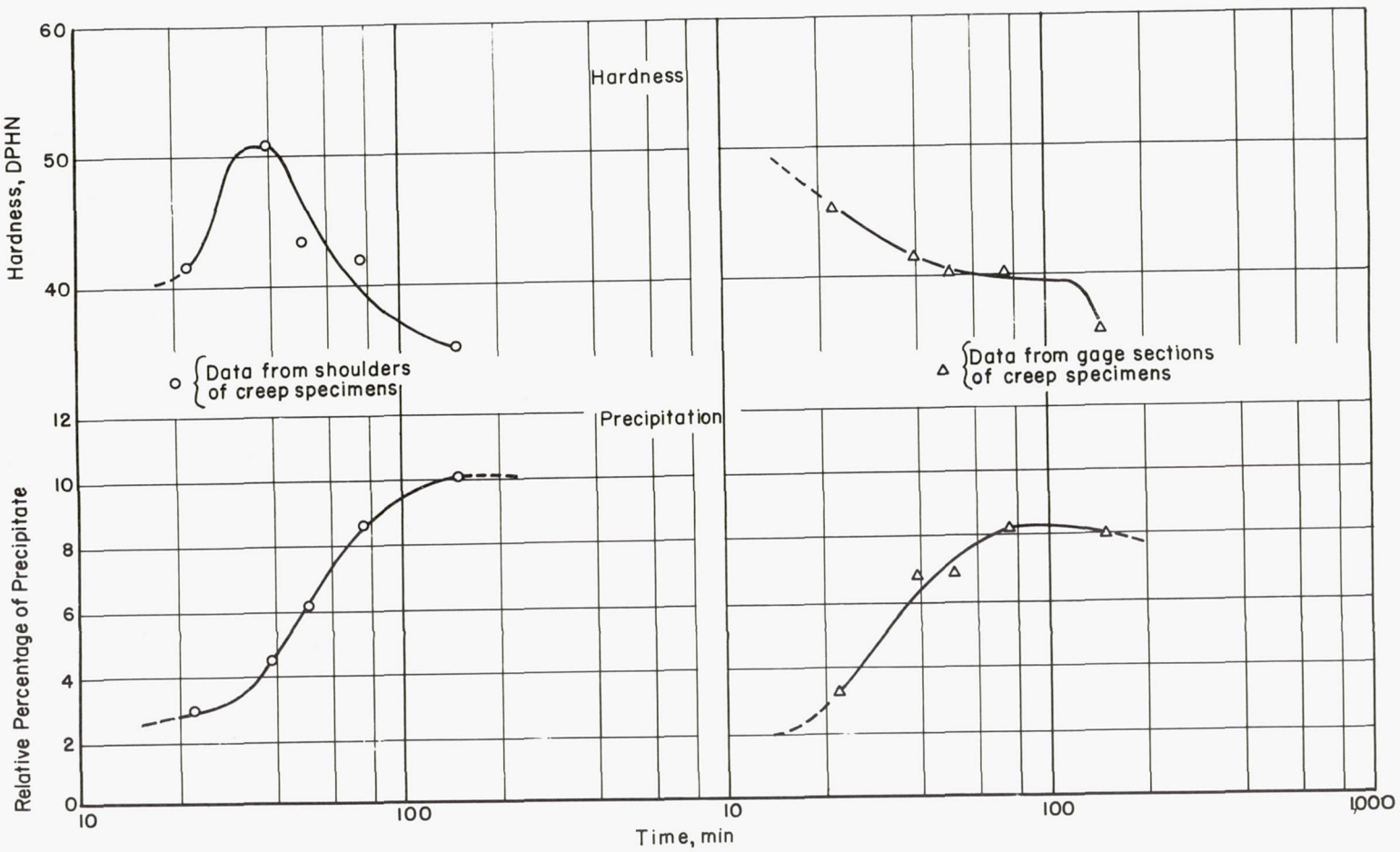

(b) Alloys crept during aging at 400° C under a stress of 1,700 psi.

Figure 17.- Concluded.

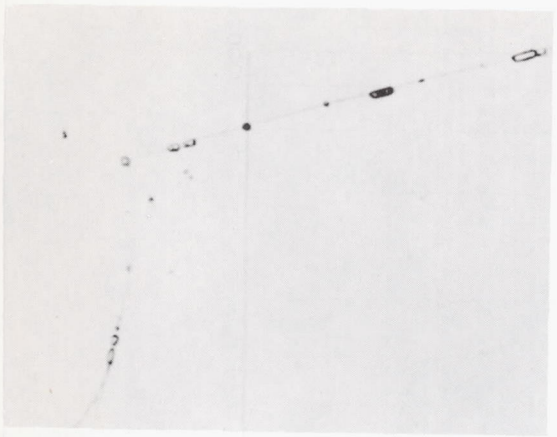

30 min

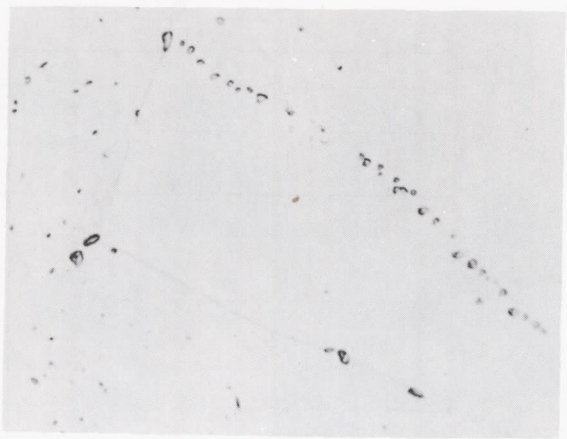

60 min

120 min

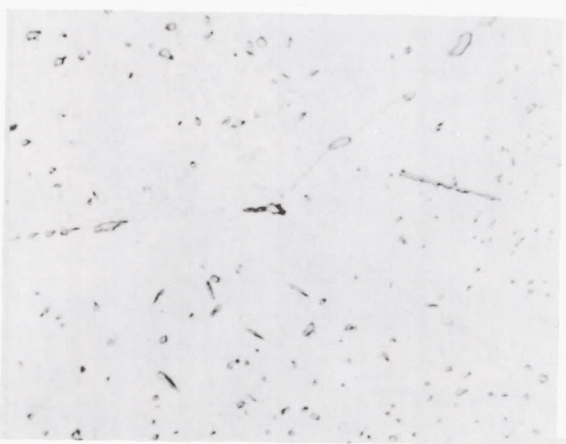

240 min

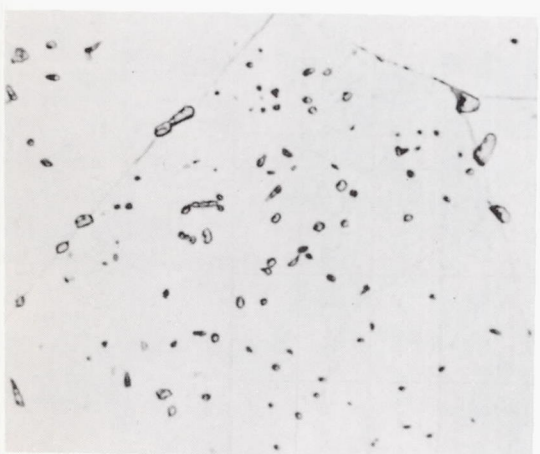

480 min

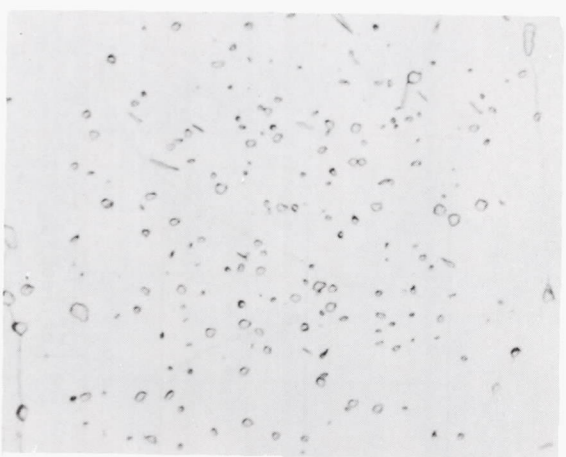

960 min

L-57-2578

Figure 18.- Precipitation in unstressed aluminum alloy containing 2 percent copper aged at 400° C for indicated times. Magnification, X1,000; Keller's etch.

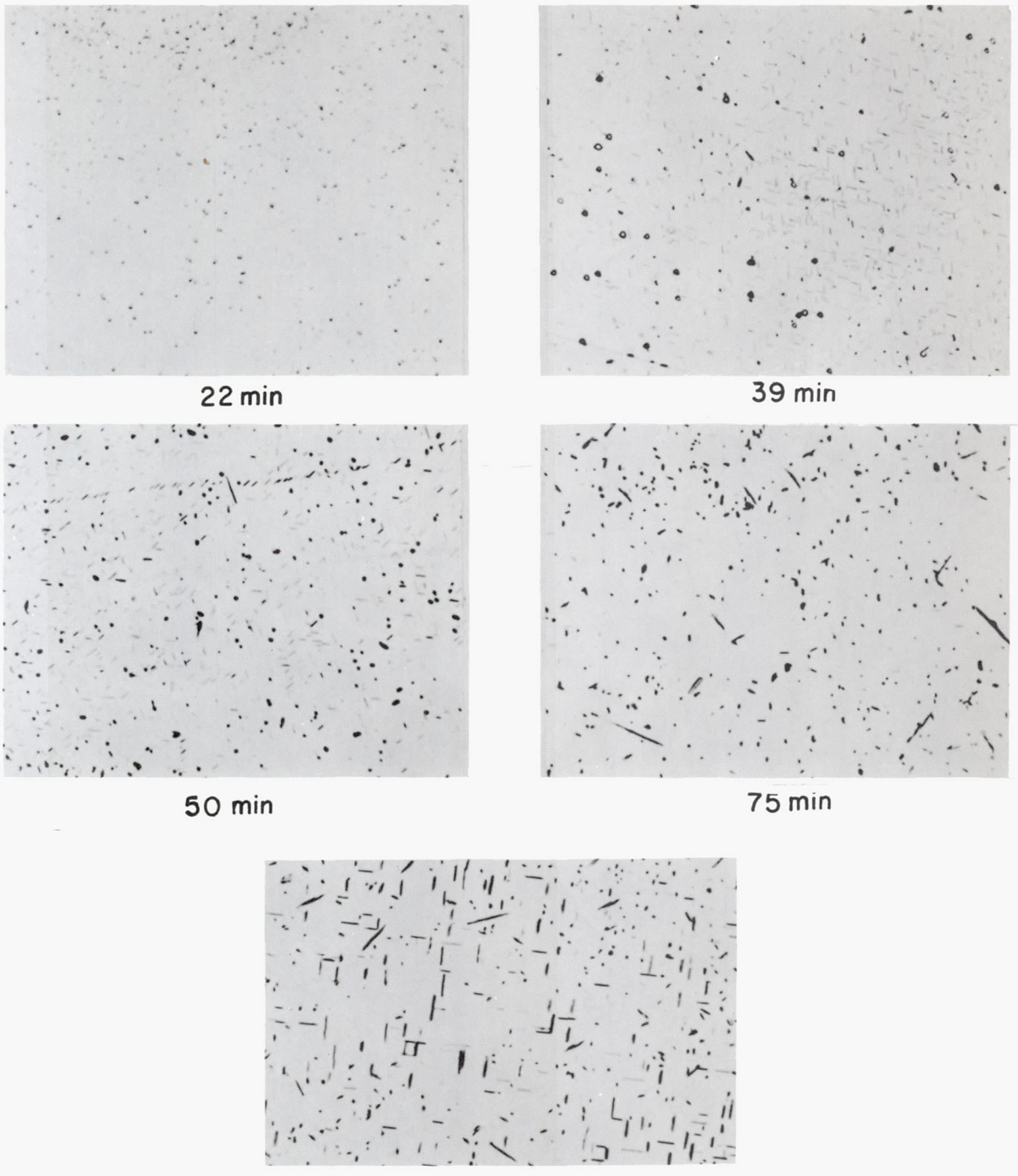

(a) Samples taken from shoulders of specimens crept for indicated times.

Figure 19.- Precipitation in aluminum alloys containing 2 percent copper crept and aged at 400° C under an initial creep stress of 1,700 psi. Magnification, X1,000; Keller's etch.

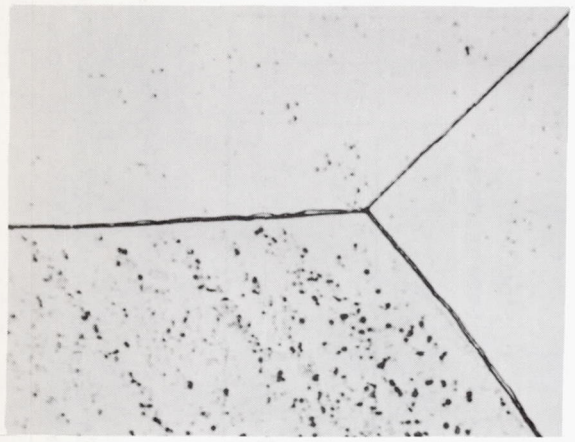

22 min

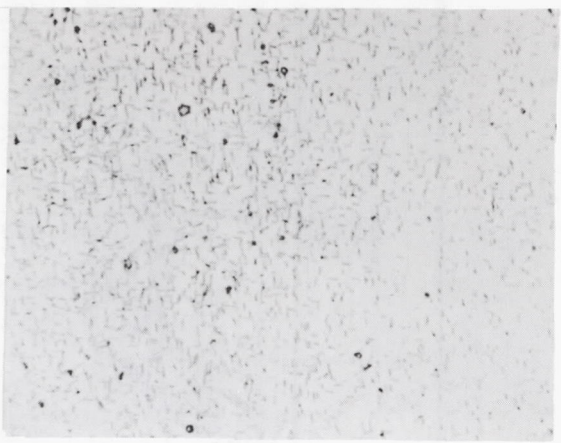

39 min

50 min

75 min

149 min

L-57-2580

(b) Samples taken from the gage sections of specimens crept for the indicated times.

Figure 19.- Concluded.

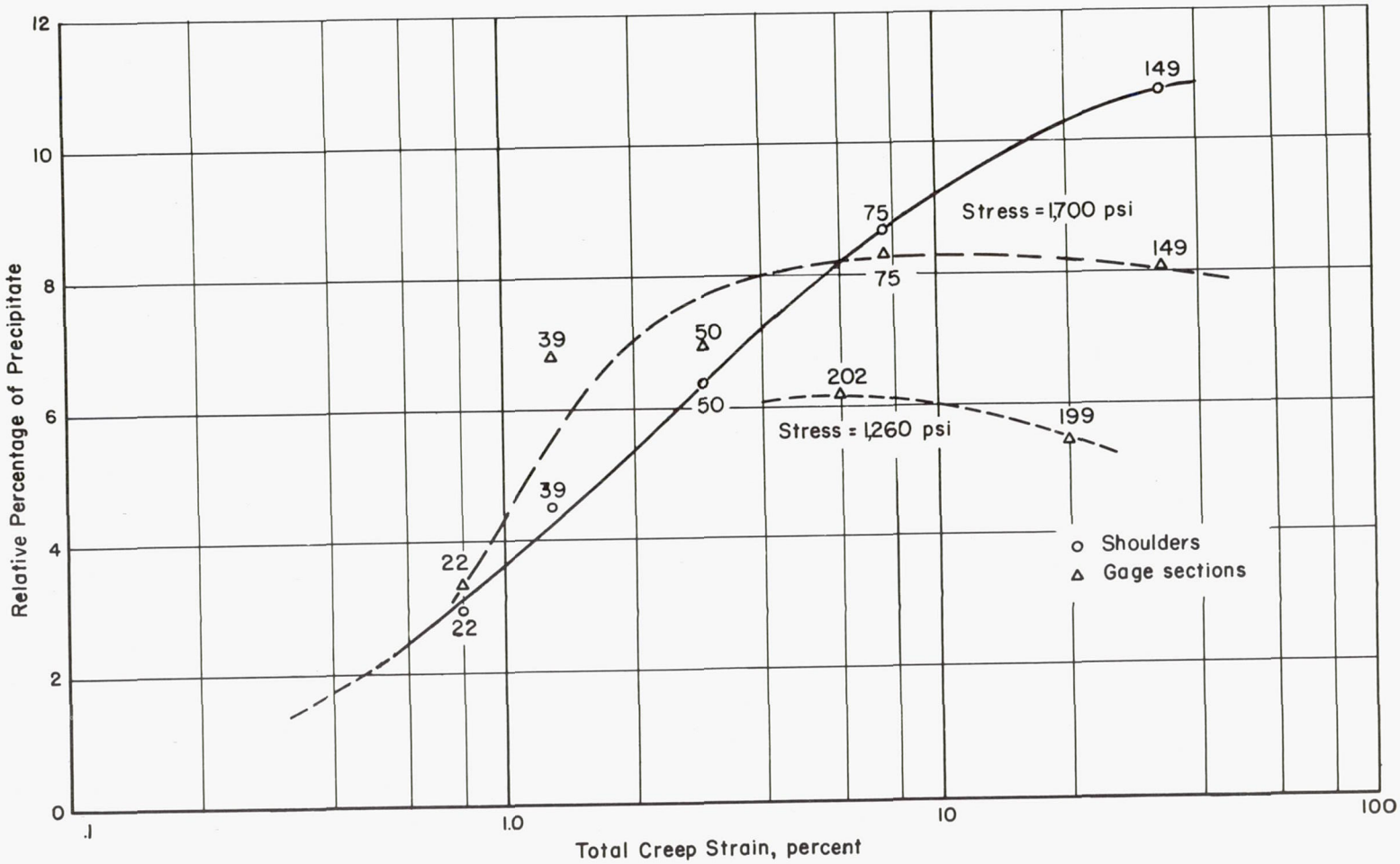

Figure 20.- Effect of stress on relative percentage of precipitate in stressed alloys containing 2 percent copper aged during creep at 400° C. Numbers at data points give duration of creep test in minutes.

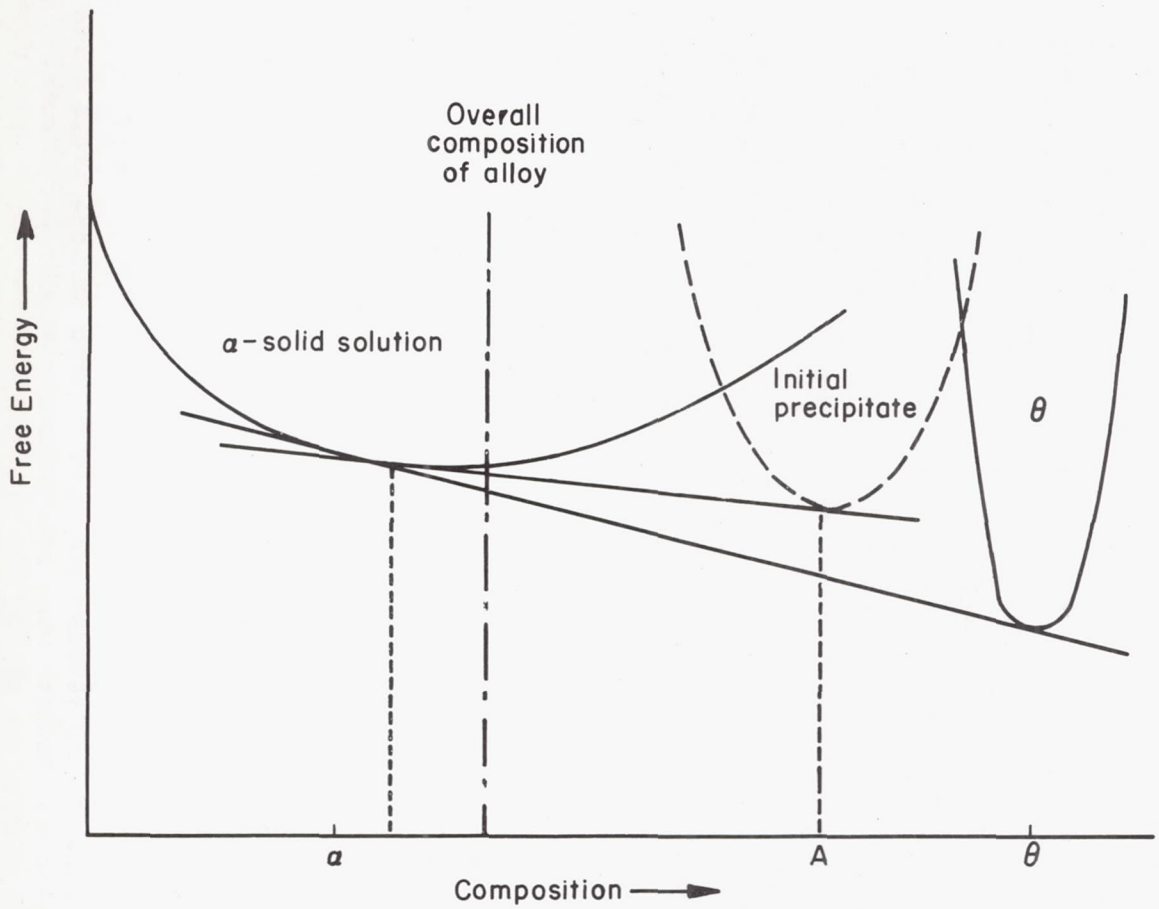

Figure 21.- Curves of hypothetical free energy against composition.

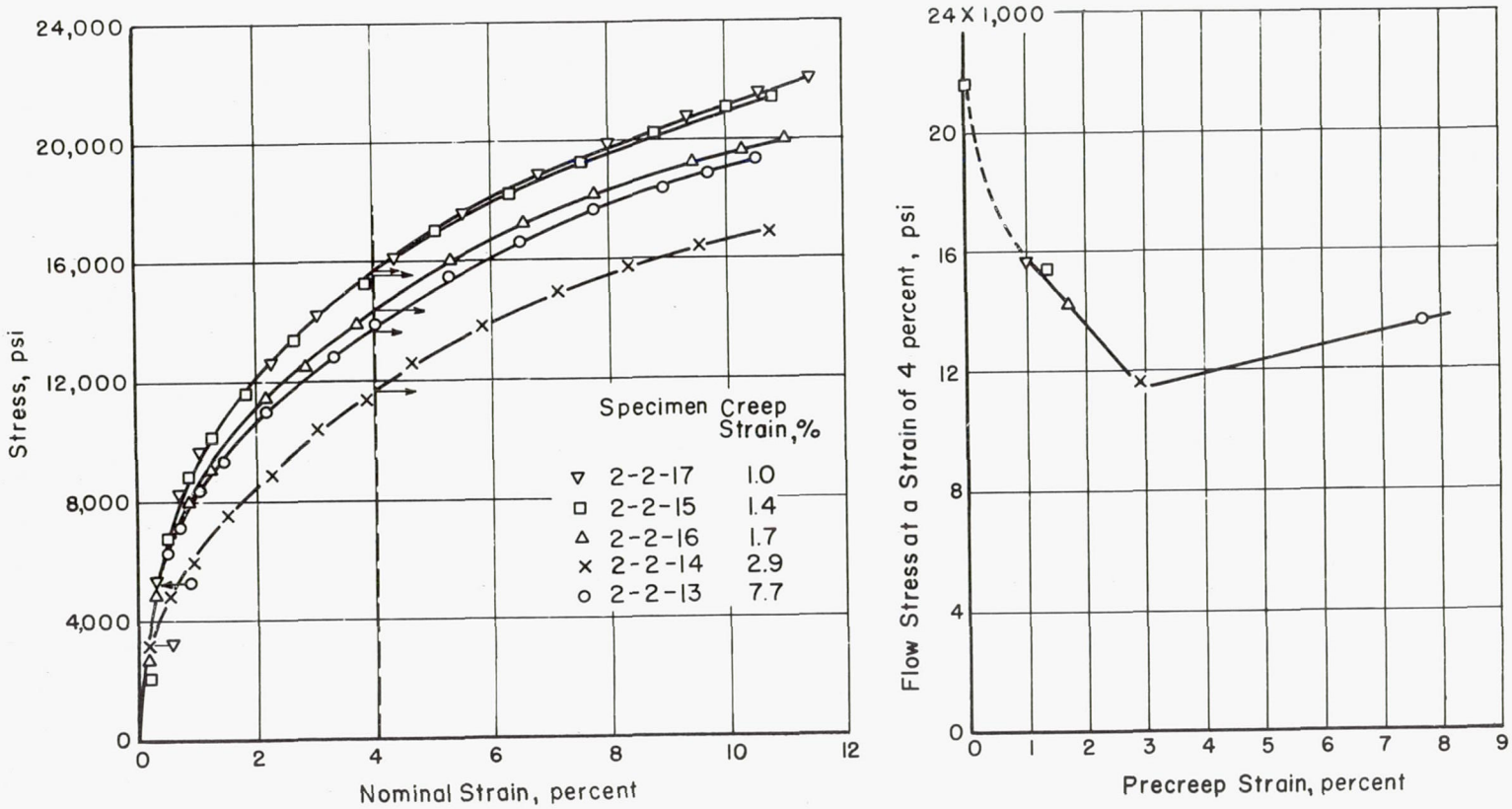

(a) Room-temperature stress-strain curves of precrept 2-percent-copper alloys. Creep stress, 790 psi; creep temperature, 400° C.

(b) Tensile flow stress $\sigma_{\epsilon=0.04}$ as a function of precreep strain (data from part (a)).

Figure 22.- Derivation of flow stress versus creep strain from stress-strain curves for aluminum-copper alloys. Strain rate, approximately 0.0078 per minute.

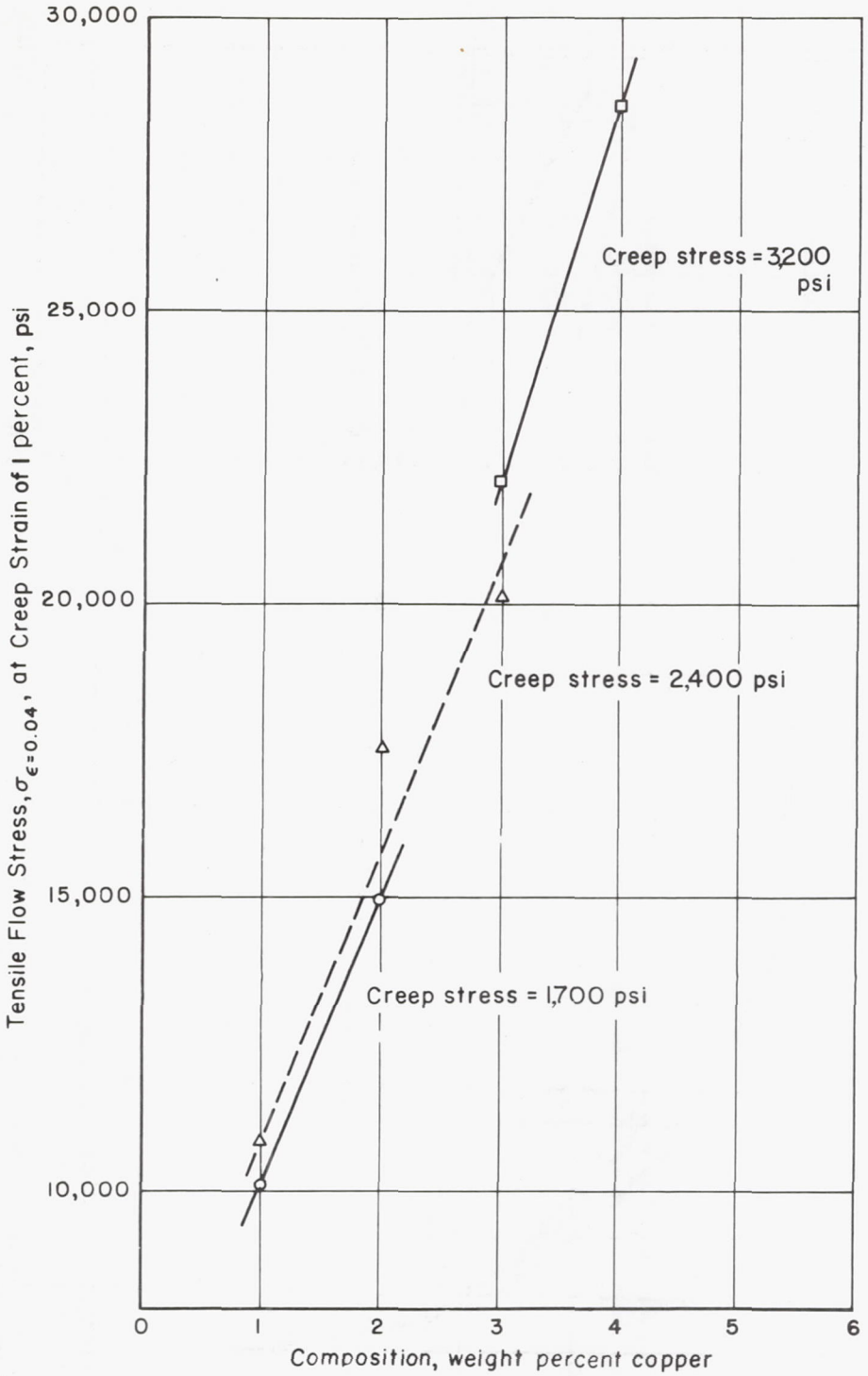

Figure 23.- Effect of composition on tensile flow stress of aluminum-copper alloys precrept to 1-percent strain at 300° C.

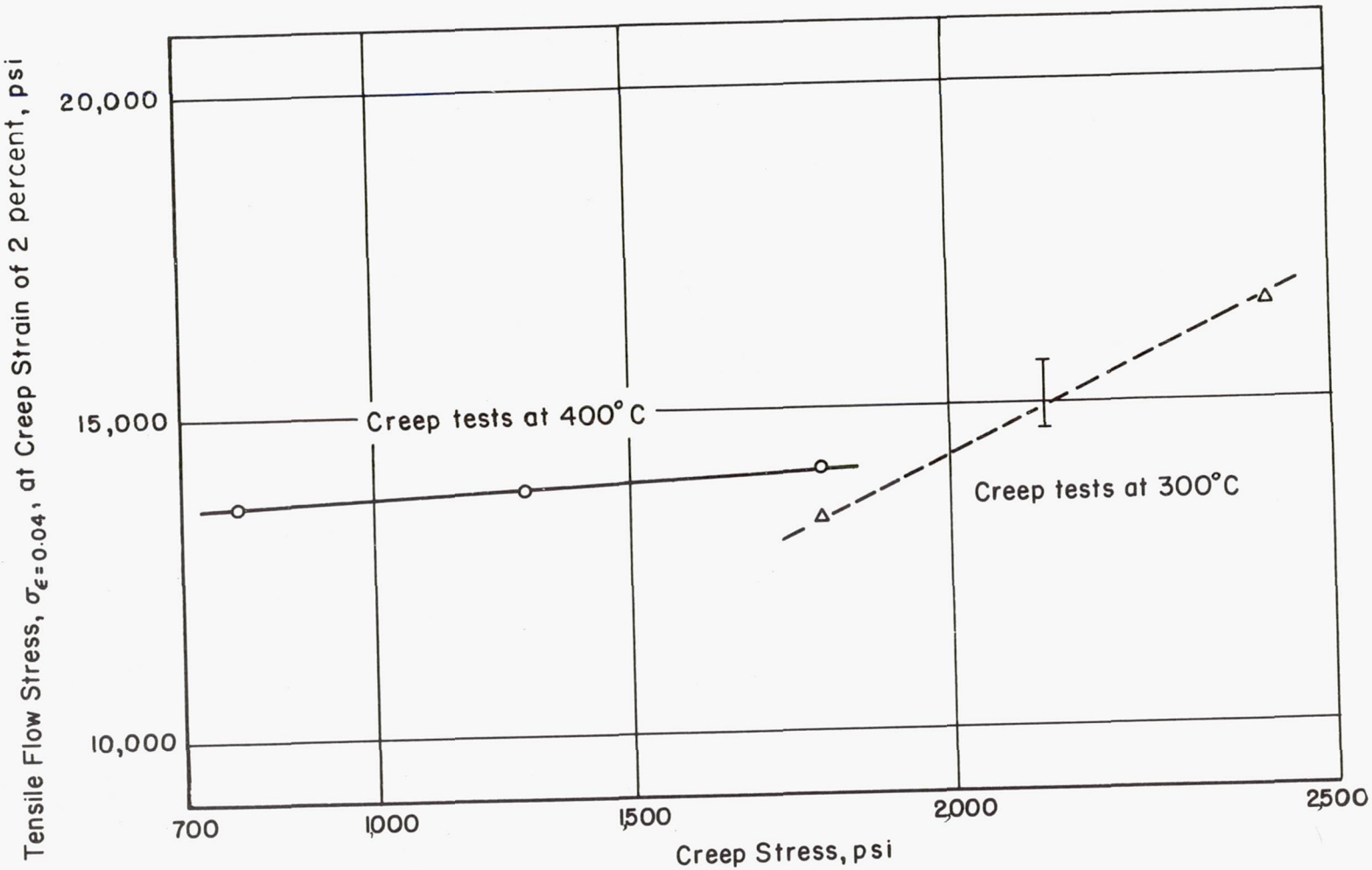

Figure 24.- Effect of creep stress on tensile flow stress of aluminum alloys containing 2 percent copper precrept to 2 percent strain at 300° and 400° C.

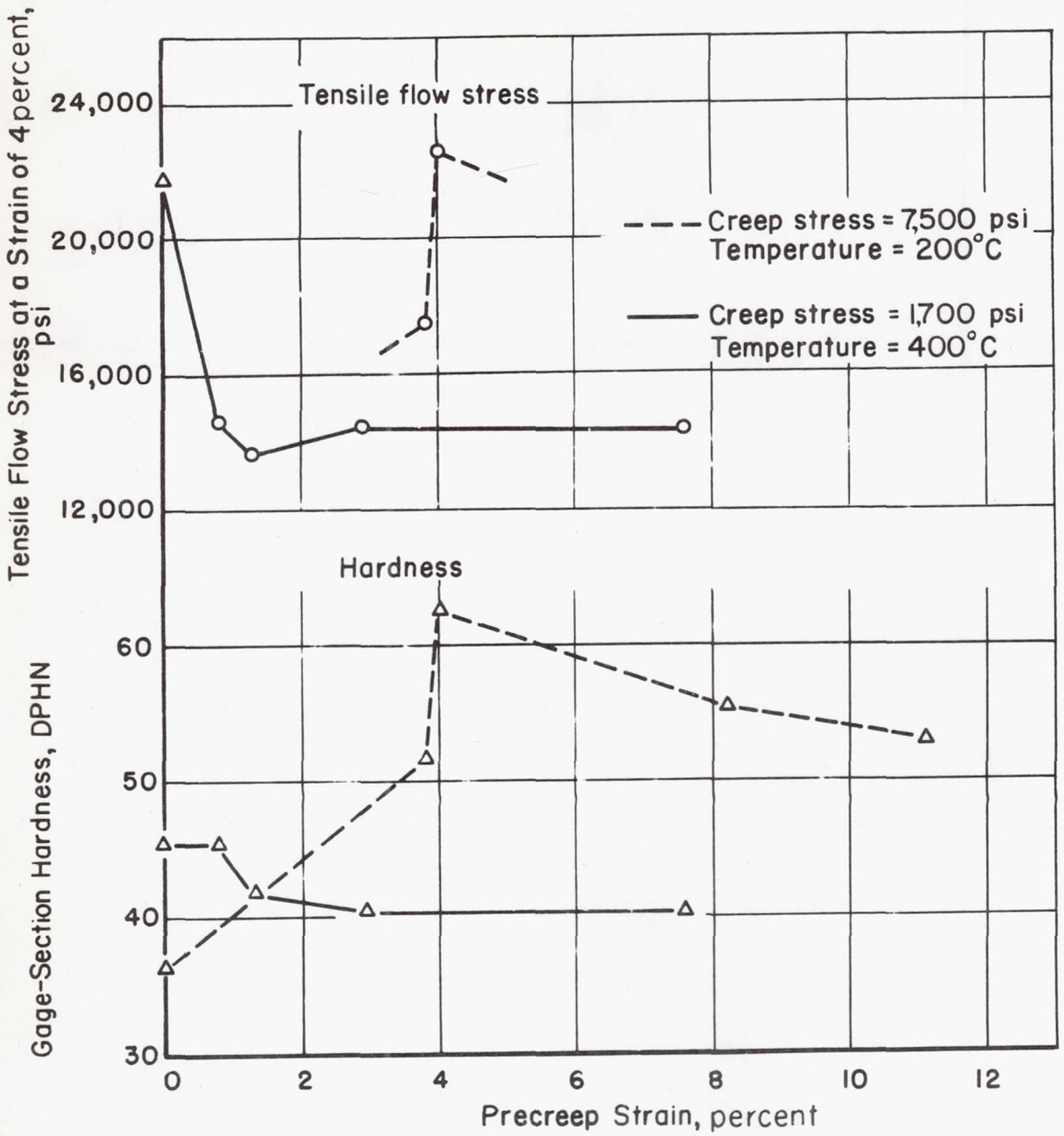

Figure 25.- Tensile flow stress at a strain of 4 percent and hardness as a function of creep strain in aluminum alloys containing 2 percent copper.

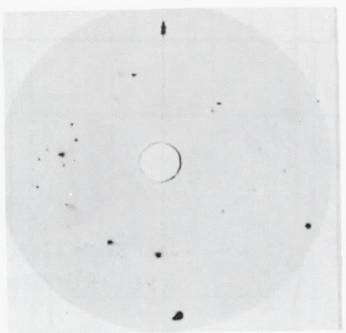

(a) Unstressed, aged $24\frac{1}{2}$ hours.

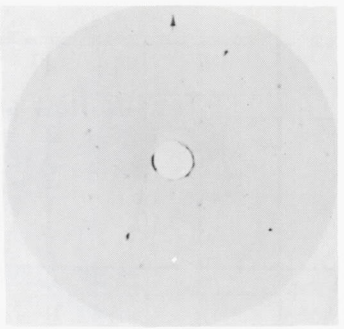

(b) Crept 22 minutes 0.80-percent strain

(c) Crept 39 minutes to 1.29-percent strain.

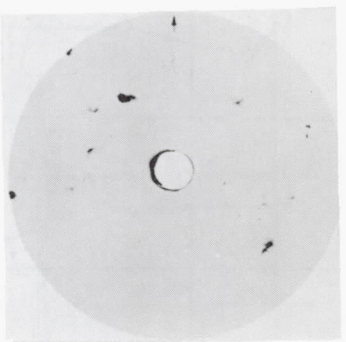

(d) Crept 50 minutes to 2.89-percent strain.

(e) Crept 75 minutes to 7.58-percent strain.

L-57-2581

(f) Crept 149 minutes to rupture at about 33-percent strain.

Figure 26.- X-ray back-reflection photographs of aluminum alloy containing 2 percent copper aged and/or stressed at 1,700 psi and 400° C. (Arrows indicate vertical direction of photographs during exposure.)

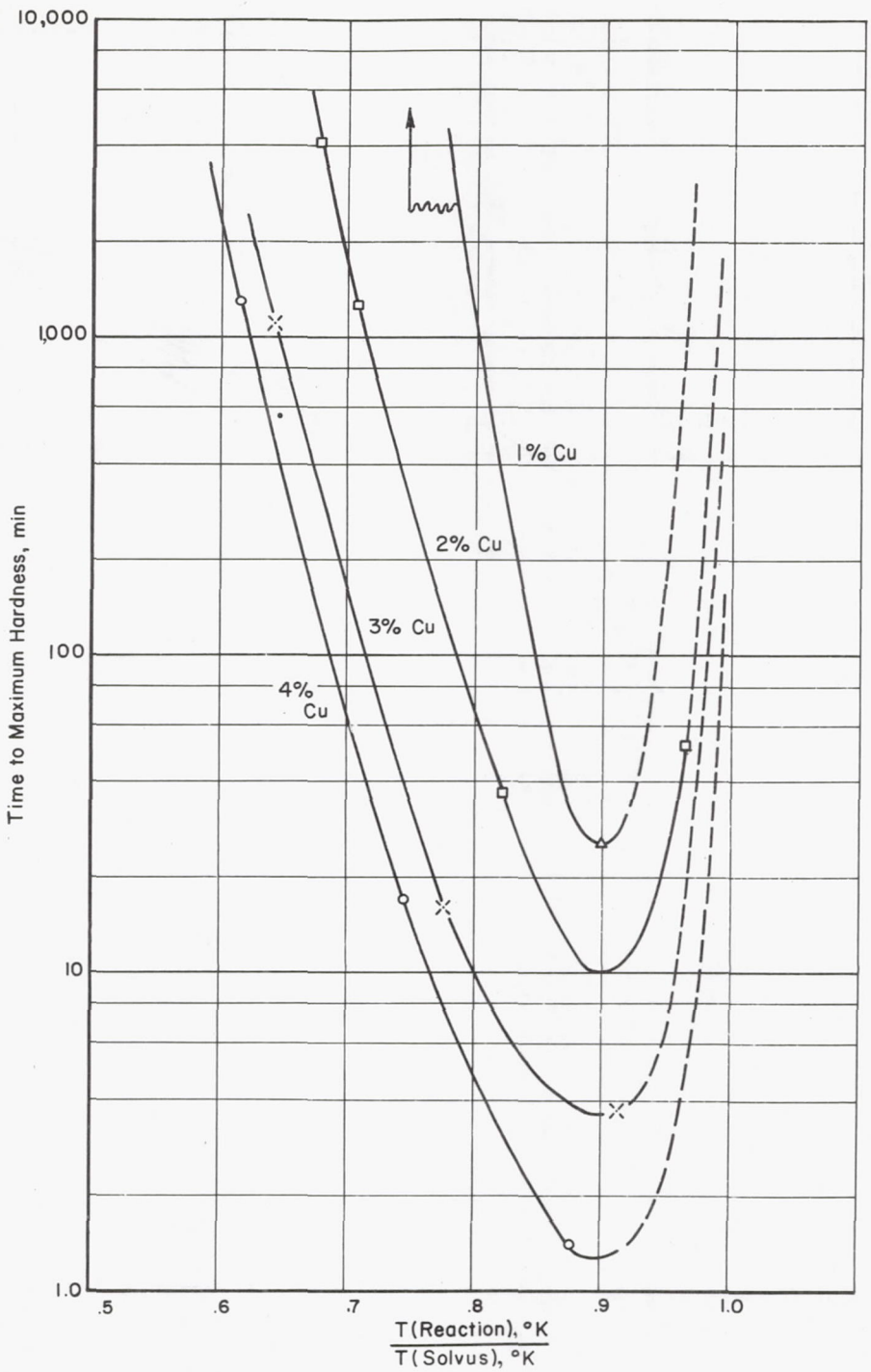

Figure 27.- Time to maximum hardness versus normalized temperature for age-hardened aluminum-copper alloys.

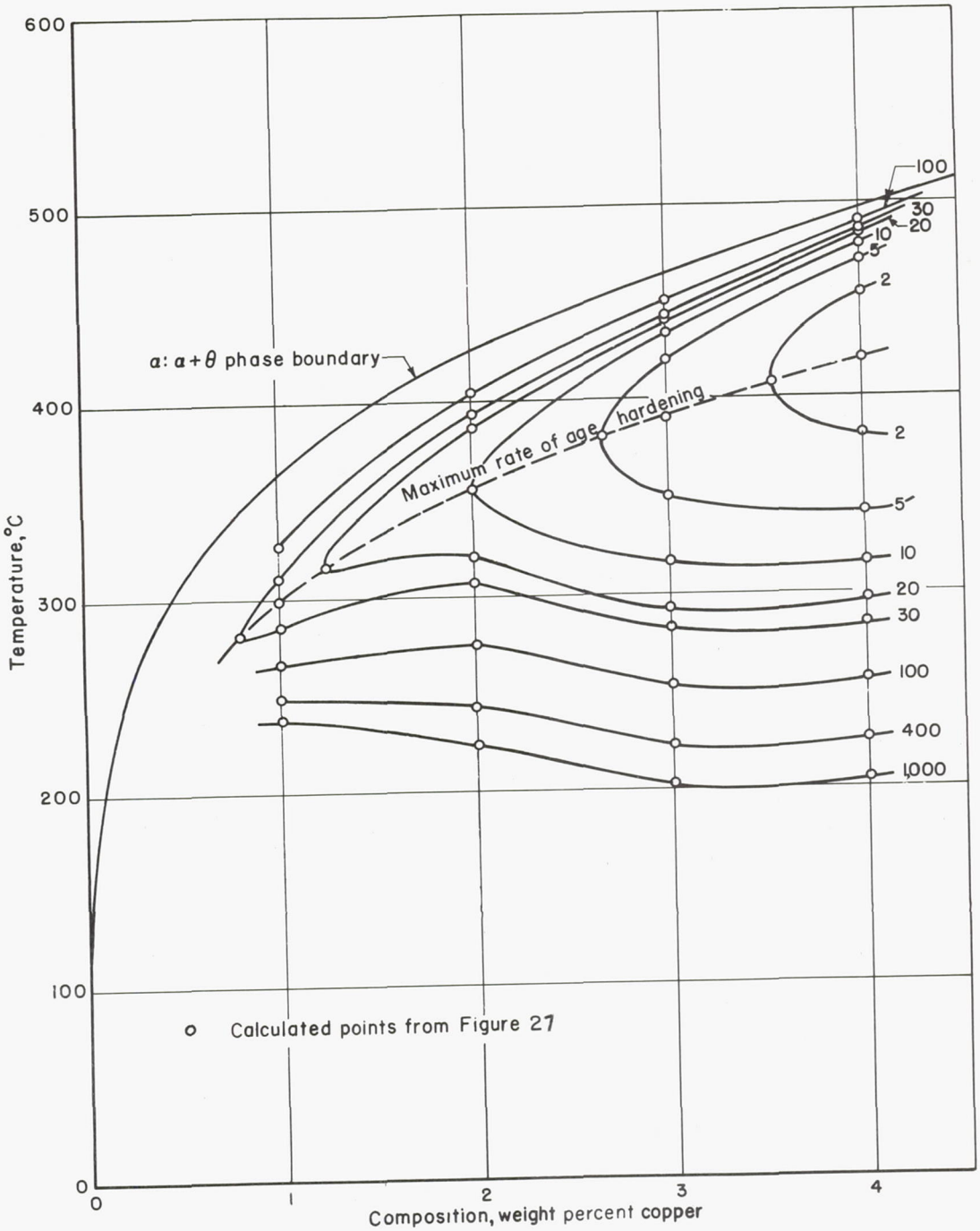

Figure 28.- Aluminum-copper equilibrium diagram, with superimposed lines of constant time-to-maximum hardness (from aging curves) and curve of maximum rate of age hardening. Numbers refer to time, in minutes, to reach maximum hardness.

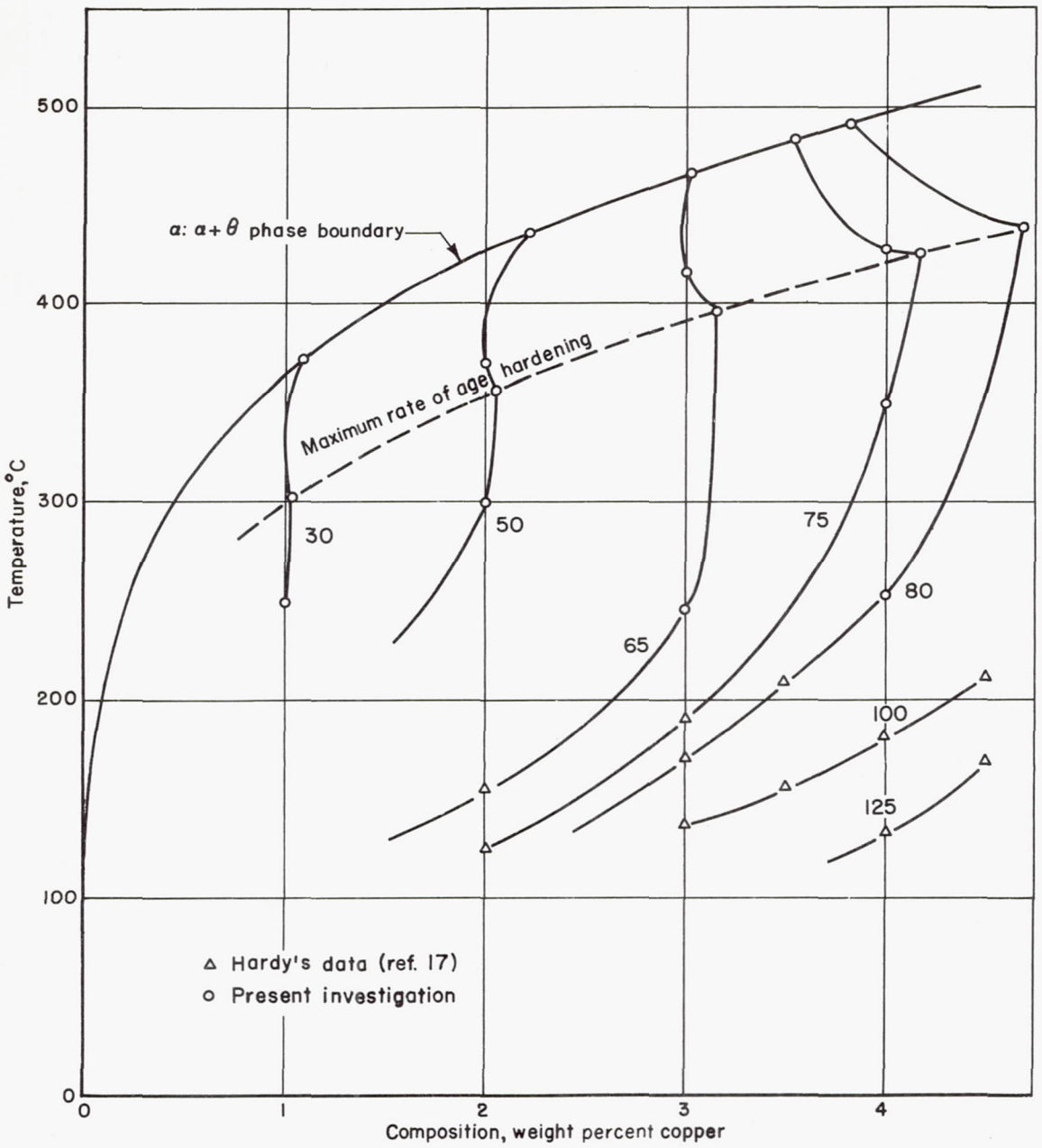

Figure 29.- Aluminum-copper equilibrium diagram showing lines of constant maximum hardness (from aging curves) and curve of maximum rate of age hardening. Numbers refer to diamond-pyramid-hardness-number hardnesses.